Large D/H variations in bacterial lipids reflect central metabolic pathways

Xinning Zhang[a], Aimee L. Gillespie[b], and Alex L. Sessions[a,b,1]

[a]Environmental Science and Engineering Program and [b]Division of Geological and Planetary Sciences, California Institute of Technology, Pasadena, CA 91125

This Feature Article is part of a series identified by the Editorial Board as reporting findings of exceptional significance.

Edited by John M. Hayes, Woods Hole Oceanographic Institution, Woods Hole, MA, and approved May 29, 2009 (received for review March 19, 2009)

Large hydrogen-isotopic (D/H) fractionations between lipids and growth water have been observed in most organisms studied to date. These fractionations are generally attributed to isotope effects in the biosynthesis of lipids, and are frequently assumed to be approximately constant for the purpose of reconstructing climatic variables. Here, we report D/H fractionations between lipids and water in 4 cultured members of the phylum *Proteobacteria*, and show that they can vary by up to 500‰ in a single organism. The variation cannot be attributed to lipid biosynthesis as there is no significant change in these pathways between cultures, nor can it be attributed to changing substrate D/H ratios. More importantly, lipid/water D/H fractionations vary systematically with metabolism: chemoautotrophic growth (approximately −200 to −400‰), photoautotrophic growth (−150 to −250‰), heterotrophic growth on sugars (0 to −150‰), and heterotrophic growth on TCA-cycle precursors and intermediates (−50 to +200‰) all yield different fractionations. We hypothesize that the D/H ratios of lipids are controlled largely by those of NADPH used for biosynthesis, rather than by isotope effects within the lipid biosynthetic pathway itself. Our results suggest that different central metabolic pathways yield NADPH—and indirectly lipids—with characteristic isotopic compositions. If so, lipid δD values could become an important biogeochemical tool for linking lipids to energy metabolism, and would yield information that is highly complementary to that provided by ^{13}C about pathways of carbon fixation.

fatty acids | fractionation | metabolism | hydrogen isotopes

The hydrogen-isotopic composition ($^2H/^1H$ or D/H ratio, commonly expressed as a δD value) of lipids is being explored by scientists with diverse interests, including the origins of natural products (1, 2), biogeochemical cycles (3), petroleum systems (4), and paleoclimate (5–7). Because the D/H ratios of lipids are generally conserved over ≈10^6-year time scales (8), they are a potentially useful tracer of biogeochemical pathways and processes in the environment. Most research to date has focused on higher plants, in which environmental water is the sole source of external hydrogen and consequently provides primary control over the D/H ratio of biosynthesized lipids (9). Although δD values for plant lipids and environmental water are generally well correlated, they are also substantially offset from each other. The biochemical basis for this lipid/water fractionation is not well understood. It is generally assumed to arise from a combination of isotope effects during photosynthesis and the biosynthesis of lipids (9–12), and is often treated as approximately constant to reconstruct isotopic compositions of environmental water as a paleoclimate proxy.

There is, however, mounting evidence that the net D/H fractionation between lipids and water can vary by up to 150‰ in plants, even in the same organism (12–16). Modest fractionations associated with fatty acid elongation and desaturation have been documented (2, 14, 15) but are unlikely to account for all of the observed variability. Recent surveys of lipids in marine environments have hinted at even greater variability in isotopic compositions. Jones et al. (17) measured fatty acids extracted from coastal marine particulate organic matter (POM) and found δD values ranging from −73 to −237‰. Measurements of lipids from marine sediments have extended this range from −32 to −348‰ for lipids with *n*-alkyl skeletons and −148 to −469‰ for those with isoprenoid skeletons (18). Because the lipids measured by both studies likely derive from marine organisms inhabiting seawater of essentially constant δD value (≈0‰), such differences cannot be due to varying environmental water. Rather, they must relate to more fundamental differences in metabolism.

Culture studies, although limited in number, support the occurrence of highly variable D/H fractionations. Hydrocarbons produced by the green alga *Botryococcus braunii* were depleted in D relative to growth water by 197 to 358‰ (16). Fatty acids from the aerobic methanotroph *Methylococcus capsulatus* (19) were depleted by 20 to 70‰, whereas those in the sulfate-reducing chemoautotroph *Desulfobacterium autotrophicum* were depleted by 190 to 360‰ (20). The most strongly fractionating organism reported to date is an H_2 + CO_2 using acetogen, *Sporomusa* sp. DSM 58, which produced fatty acids with depletions in D of nearly 400‰ (21).

Some of this reported variability can be ascribed to systematic differences between lipids with *n*-alkyl versus isoprenoid skeletons. Isoprenoid lipids are typically D depleted relative to *n*-alkyl lipids by 100‰ or more, a pattern now widely confirmed in both culture (13, 16, 19) and environmental samples (12, 18). However, significant variability within single classes of lipids (e.g., fatty acids) cannot be explained because the chemical mechanisms of lipid biosynthesis are strongly conserved across most bacterial and eukaryotic phyla (22–25). Thus, many important questions linger. Do D/H fractionations associated with different metabolic lifestyles (i.e., photoautotrophy, chemoautotrophy, or heterotrophy) systematically differ? Do they differ in bacteria versus eukaryotes? Perhaps most fundamentally, how and why do biosynthetic processes fractionate hydrogen isotopes at the molecular level and lead to lipids with such diverse isotopic compositions? These questions lie at the heart of our ability to use and interpret lipid δD values from all types of environmental samples. To explore such issues, we measured lipid D/H fractionations in 4 metabolically versatile bacteria grown under photoautotrophic, photoheterotrophic, chemoautotrophic, and heterotrophic conditions on a range of carbon sources metabolized by different pathways of central metabolism.

Results

Cultures and Fatty Acids. Four species of bacteria, chosen to provide a sampling of metabolic diversity, were grown in batch

Author contributions: X.Z. and A.L.S. designed research; X.Z., A.L.G., and A.L.S. performed research; X.Z. analyzed data; and X.Z. and A.L.S. wrote the paper.

The authors declare no conflict of interest.

[1]To whom correspondence should be addressed. E-mail: als@gps.caltech.edu.

This article contains supporting information online at www.pnas.org/cgi/content/full/0903030106/DCSupplemental.

Table 1. Summary of culture experiments

Organism-substrate	δD_s,* ‰	δD_w,† ‰	Growth rate,‡ h^{-1}	Cultures§
C. oxalaticus				
oxalate	—	−68.6 to +218.3	0.29	Co1-I,II,III,IV
oxalate	—	−68.6 to +218.3	0.28	Co2-I,II,III,IV
formate	972	−68.6 to +218.3	0.33	Co3-I,II,III,IV
acetate	−76	−68.6 to +218.3	0.50	Co4-I,II,III,IV
succinate	−97	−64.3 to +214.1	0.60	Co5-I,II,III,IV
succinate	−97	+41.1 to +214.1	NA	Co6-II,III,IV
C. necator				
formate	972	−68.3	0.17	Cn1-I
fructose	−22	−65.5	0.34	Cn2-I
gluconate	NA	−68.1	0.36	Cn3-I
pyruvate	−12	−64.4	0.61	Cn4-I
acetate	−76	−68.5	0.35	Cn5-I
succinate	−97	−68.6	0.48	Cn6-I
succinate	−97	−68.6	NA	Cn7-I
E. coli				
glucose	−60	−61.9	0.64	Ec1-I
gluconate	NA	−62.2	0.57	Ec2-I
pyruvate	−12	−68.1	0.37	Ec3-I
acetate	−76	−62.4	0.31	Ec4-I
glucose	−60	−60.0 to +314.0	0.66	Ec5-I,II,III,IV
LB	NA	−60.0 to +152.0	NA	Ec6-I,II,III
R. palustris				
acetate	NA	−53.6	0.10	Rp1-I
acetate, light	NA	−53.6	0.068	Rp2-I
CO_2, light	—	−53.6	0.015	Rp3-I

*δD of non-exchangeable C-bound H in the growth substrate (see *SI Methods* for calculation details). Uncertainties are likely < 20‰. − indicates a substrate with no H, NA, not available.
†δD of culture medium before inoculation. Average analytical uncertainty (1σ) is 0.7‰. Range refers to the span of values covered by 4 replicate cultures, each differing by ≤100‰.
‡1σ was ≤0.04 for $n \geq 2$ cultures in experiments Co1-Co5.
§Multiple numbers indicate parallel cultures grown in medium with different δD_w values. Cultures Co6-II,III,IV and Cn7-I were harvested in stationary phase, all others were harvested in exponential phase. OD values at harvest are in Fig. S1.

culture on varying substrates (Table 1, see *SI Methods* for details). *Cupriavidus oxalaticus* str. OX1 and *C. necator* str. H16 are facultative chemoautotrophic *β-Proteobacteria* commonly found in soil and freshwater environments (26), and were grown as aerobic heterotrophs and chemoautotrophs. The model organism *Escherichia coli* K-12 str. MG1655, an obligate heterotrophic γ-Proteobacterium, was grown aerobically. The purple non-sulfur anoxygenic phototroph *Rhodopseudomonas palustris* str. TIE-1 is an α-Proteobacterium and was grown under anaerobic photoautotrophic, anaerobic photoheterotrophic, and aerobic heterotrophic conditions. Organic substrates were chosen based on their catabolic relationship to the different pathways of central metabolism. They include those that feed into glycolysis (glucose, fructose, gluconate, pyruvate), the tricarboxylic acid (TCA) cycle (acetate, succinate), and chemoautotrophic* metabolism [formate, oxalate (27–29)].

Most cultures were harvested during exponential growth (Fig. S1). Fatty acids were solvent-extracted, derivatized as methyl esters, and quantified by gas chromatography/mass spectrometry (GC/MS; Table S1). The most abundant fatty acids in *C. oxalaticus* and *C. necator* were palmitic (16:0), palmitoleic (16:1), and oleic (18:1) acids. An additional fatty acid, cyclopropyl-heptadecanoic acid (cyc-17), was abundant in *E. coli*. *R. palustris* produced significant amounts of 18:1, 18:0 (stearic acid), and 16:0 fatty acids. Relative abundances of fatty acids varied by <35% between cultures of each bacterial species, with no systematic relationship between growth substrate and fatty acid abundance (Table S1).

Values of δD for individual fatty acids varied widely between cultures (−362 to +331‰), but typically by less than ≈30‰ between different fatty acids from the same culture (Table S2). For simplicity we report and discuss the δD values for palmitic acid as representative of each culture, both because it was present in every organism and because it was generally the most abundant fatty acid.

Growth on Different Substrates Leads to Varying Fractionation Between Lipids and Water. Fig. 1 summarizes current and previous culture data and shows that the net D/H fractionations between lipids and culture water vary in all analyzed strains. The 2 *Cupriavidus* strains, which have the most metabolically versatile carbon metabolisms, exhibited the largest variability (up to 500‰). This is the largest range of isotopic fractionations yet recorded for any individual organism, and includes instances of both D enrichment and D depletion relative to water. The observed range of fractionations is substantially larger than has been previously observed in environmental samples, and—if expressed in nature—would have the potential to explain all such environmental D/H variability. At the same time, lipid/water fractionation during anoxygenic photoautotrophic growth of *R. palustris* was within the range commonly observed for plants. For

*Growth on oxalate is classically regarded as heterotrophic, not chemoautotrophic, metabolism. However, conservation of energy during growth is similar to that on formate in that 1-carbon reactions form the basis for generation of reducing power, analogous to "true" chemoautotrophy (e.g., growth on H_2 + CO_2) (29, 30). Hence we refer here to growth on formate and oxalate as chemoautotrophic for the purpose of describing hydrogen, rather than carbon, metabolism.

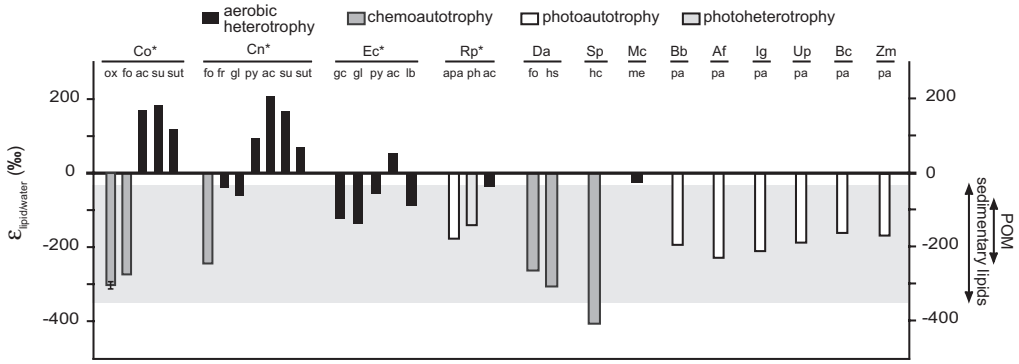

Fig. 1. Summary of D/H fractionations between fatty acids and water observed in culture experiments, native specimens, and marine organic matter fractions. Plotted fractionations are based on the average δD value of palmitic acid, or the fatty acid/alkane of nearest chain length, in the culture with water δD closest to 0‰. Bacterial cultures from this study (*) are *C. oxalaticus* (Co), *C. necator* (Cn), *E. coli* (Ec), and *R. palustris* (Rp). Organisms from other studies (13, 16, 19–21, 61) are cultured bacteria *D. autotrophicum* (Da), *Sporumusa* sp. (Sp), and *M. capsulatus* (Mc), cultured phytoplankton *B. braunii* (Bb), *Alexandrium fundyense* (Af), *Isochrysis galbana* (Ig), and natural specimens of brown alga *Undaria pinnatifida* (Up), red alga *Binghamia californica* (Bc), and seagrass *Zostera marina* (Zm). The gray box covers the range of fractionations observed in marine POM and sediments (17, 18). Growth substrates are oxalate (ox), formate (fo), fructose (fr), glucose (gc), gluconate (gl), pyruvate (py), acetate (ac), succinate (su, sut), LB (lb), $H_2 + CO_2$ (hc), $H_2 + SO_4^{2-}$ (hs), methane (me), acetate+light (ph), CO_2 + light (pa), $S_2O_3^{2-} + CO_2$ + light (apa). Error bars for culture Co*-ox are the standard deviation ($\pm 1\sigma$) for 4 sets of biological replicates; other cultures were not replicated. Typical analytical uncertainties are ± 3.5‰ for all cultures.

heterotrophic cultures, the δD values of most supplied organic substrates (δD_s) differ by <100‰ (Table 1) and cannot explain the range of observed lipid δD values. For example, growth of *E. coli* on glucose ($\delta D_s = -60‰$) led to D depletion of lipids relative to both water and substrate, whereas growth on acetate ($\delta D_s = -76‰$) led to D enrichment.

Our data show a strong correspondence between the pathways of substrate metabolism and lipid δD values. Growth on formate or oxalate, catabolized through 1-carbon reactions (29, 30), yielded lipids depleted in D by 200 to 300‰ relative to water (Fig. 1, Table S2). Heterotrophic growth on sugars and photoautotrophic growth on CO_2 produced lipids depleted by 50 to 190‰ relative to water. Growth on a direct precursor (acetate) and intermediate (succinate) of the TCA cycle yielded lipids that were generally D-enriched relative to water (−50 to +200‰), with growth phase modulating the level of enrichment (compare "su" vs. "sut" in Fig. 1). These patterns are most strongly exhibited in the 2 *Cupriavidus* strains, but are also present in *E. coli* and *R. palustris*.

Manipulation of Growth Water δD: Fractionation Factor Curves. Additional information on the biochemical causes of these variable fractionations can be deduced from experiments in which the isotopic composition of culture water is experimentally manipulated (19). Conceptually, the net fractionations between lipids and each external H source (i.e., water and organic substrate) can be treated as distinct, yielding the isotopic mass balance

$$R_l = X_w \alpha_{l/w} R_w + (1 - X_w)\alpha_{l/s} R_s, \quad [1]$$

where R_l, R_w, and R_s denote the D/H ratios of lipids, water, and substrates, respectively (31). X_w is the mole fraction of lipid H derived from external water, whereas $\alpha_{l/w}$ and $\alpha_{l/s}$ represent the net isotopic fractionations associated with uptake and utilization of water and substrate hydrogen, respectively. Eq. **1** represents the overall isotopic relationship between lipids and external sources of H, and does not imply that the sources must be directly involved in lipid biosynthesis (e.g., glucose may contribute H to lipids by way of metabolic intermediates even though it does not directly participate in the biosynthetic reactions). Measurements of R_w, R_s, and R_l for parallel cultures in which only 1 parameter, R_w, is varied experimentally form the basis for regression of R_l on R_w. This yields a unique slope and intercept that can be used to constrain the relevant fractionations.

To this end, *C. oxalaticus* and *E. coli* were grown on glucose, acetate, succinate, formate, oxalate, and Lysogeny broth (LB) using waters with δD values ranging from −68 to +314‰. Strong linear relationships ($R^2 \geq 0.98$) between δD values of fatty acids and water were obtained for all such experiments (Fig. 2), implying that the uncertainty in δD values for each culture is minimal (probably <20‰). This is consistent with several "true" biologic replicates grown in identical waters, for which δD values differed by <11‰ (1σ).

For cultures where X_w is known, $\alpha_{l/w}$ and $\alpha_{l/s}$ can be calculated directly from the slope and intercept of the regression. Oxalate carries no H at physiological pH, so $X_w = 1$ for *C. oxalaticus* growing on oxalate. The corresponding value of $\alpha_{l/w}$ ranged from 0.64 to 0.73 for different fatty acids (Table S3). Growth on formate yielded nearly identical results, even though formate is

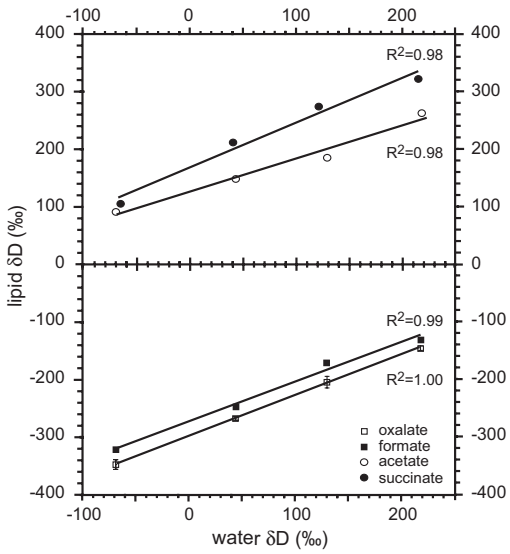

Fig. 2. Regressions of δD values for palmitic acid versus water for *C. oxalaticus* grown on oxalate, formate, acetate, and succinate. Error bars represent 1σ uncertainty for biological replicates. Data for other lipids are in Fig. S2 and Table S3. Each regression provides constraints on fractionations that can be described most succinctly as a single fractionation curve (see Fig. 3).

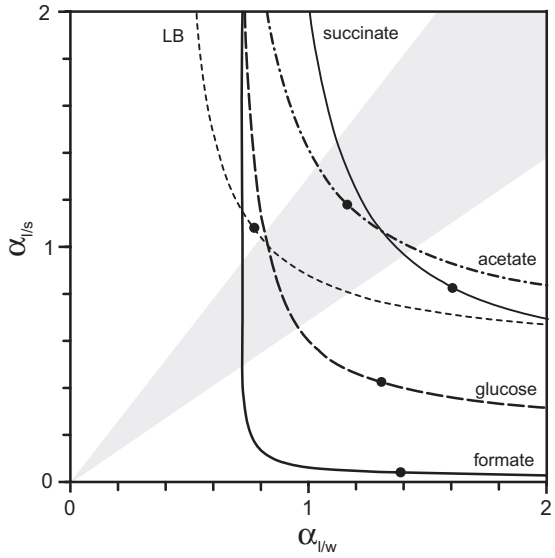

Fig. 3. Fractionation factor curves for palmitic acid in *C. oxalaticus* grown on formate, acetate, and succinate, and in *E. coli* grown on glucose and LB. Each curve represents the set of all possible combinations of $\alpha_{l/s}$ and $\alpha_{l/w}$ satisfying the constraints imposed by parallel cultures with differing R_w (i.e., 1 linear regression in Fig. 2). Filled circles indicate values corresponding to $X_w = 0.5$. Gray shaded area defines up to 600‰ variation between $\alpha_{l/s}$ and $\alpha_{l/w}$. Increases in the true value of $\alpha_{l/s}$, $\alpha_{l/w}$, and X_w shift curves up, to the right, or down a diagonal as detailed in Fig. S3.

a potential source of H. We infer that H on formate exchanges with water to preclude the transmission of substrate H to fatty acids, in accord with our understanding of formate metabolism (29) and the recent results of Campbell et al. (20).

If X_w is unknown, as is the case for most heterotrophic growth conditions, then a unique solution for X_w, $\alpha_{l/w}$, and $\alpha_{l/s}$ is not possible (31). However, the results of each regression can be depicted as a curve relating $\alpha_{l/s}$ to $\alpha_{l/w}$, with each point on the curve representing a different possible combination of values for X_w, $\alpha_{l/w}$, and $\alpha_{l/s}$ (Fig. 3). These relationships, which we term "fractionation curves," are unique for each set of culture conditions and provide a useful means for comparison even while the true values of X_w, $\alpha_{l/w}$, and $\alpha_{l/s}$ remain unknown. A basic understanding of the behavior of such curves aids in their interpretation: When comparing 2 fractionation curves, representing 2 different culture conditions, an increase in the true value of $\alpha_{l/w}$ between conditions will shift the curves horizontally to the right; an increase in the true value of $\alpha_{l/s}$ will shift them vertically upward; and an increase in X_w will shift them diagonally downward and to the right (see Fig. S3).

Two key inferences can be drawn from the fractionation curves in Fig. 3. First, within a plausible range of values for the 2 fractionation factors (0.5 to 2.0), equivalent to ± 1,000‰ and 2-fold larger than any net fractionations yet measured for biosynthetic processes, many fractionation curves do not intersect. This is possible only if both $\alpha_{l/w}$ and $\alpha_{l/s}$ vary between conditions (e.g., compare *C. oxalaticus* on formate vs. *E. coli* on glucose vs. *C. oxalaticus* on succinate). Changes in fractionation associated with the assimilation of substrate, $\alpha_{l/s}$, cannot by itself explain our results, and it is clear that the concept of a nearly constant lipid/water fractionation must be discarded. Because $\alpha_{l/w}$ changes even in a single organism, whereas pathways of lipid biosynthesis are not known to change significantly with growth on different substrates, we infer that the magnitude of $\alpha_{l/w}$ is not set primarily by lipid biosynthetic reactions.

Second, fractionation curves for *E. coli* growth on glucose and LB are offset along a diagonal, and thus are likely related by similar fractionations (α values) with a decrease in X_w from glucose to LB. This is consistent with the assimilation of preformed cell constituents by cells grown on the complex LB medium, leading to smaller X_w. Curves for growth on acetate and succinate also appear related by similar fractionations with a decrease in X_w from succinate to acetate, and are consistent with the role of acetate as a direct precursor for lipid biosynthesis.

Similarity of Lipid-Substrate and Lipid-Water Fractionations. Although it is convenient to treat the net lipid/water and lipid/substrate fractionations as independent, this distinction is probably artificial. Approximately 3/4 of fatty acid H derives from central metabolites (acetate or NADPH; see *Discussion*). H derived from water and growth substrates is comingled in these and virtually all other metabolites because many common classes of reactions (isomerization, hydrolysis, rearrangement, exchange) lead to significant scrambling of C-bound H (32). At this point the 2 "external" sources of H should be affected by many of the same reactions and thus the same isotope effects. The possibility of markedly different values for $\alpha_{l/s}$ and $\alpha_{l/w}$ is therefore difficult to envision. Indeed, having widely different fractionations for water and substrate H would practically require that these two H pools remain metabolically distinct, but they do not. Although a strong covariance of $\alpha_{l/w}$ and $\alpha_{l/s}$ does reduce the utility of our isotopic labeling approach, there is also a substantial benefit in that the inverse problem—inferring biochemical processes from measured lipid δD values—is made much easier. The strong correspondence of metabolic pathways and lipid δD values implied by Fig. 1 would be highly improbable if $\alpha_{l/s}$ and $\alpha_{l/w}$ both varied widely and independently.

To extract further insight from Fig. 3, we therefore assume that $\alpha_{l/s}$ and $\alpha_{l/w}$ for any single culture differ from each other by ≤600‰ (i.e., within the gray region in Fig. 3). This is an arbitrary limit, chosen to encompass the ≈500‰ range of fractionations we observe, but more conservative limits would yield similar conclusions. Probable limits for X_w, $\alpha_{l/w}$, and $\alpha_{l/s}$ can then be calculated: formate (>95%, 0.73, NA), glucose (68–80%, 0.80–0.95, 0.67–1.05), LB (33–47%, 0.80–1.15, 0.82–1.05), succinate (58–70%, 1.13–1.38, 0.98–1.48), and acetate (40–56%, 1.03–1.43, 1.0–1.35). The fact that both $\alpha_{l/w}$ and $\alpha_{l/s}$ vary from D depletion ($\alpha < 1$) to D enrichment ($\alpha > 1$) strongly supports our contention that variability in fatty acid δD values cannot be explained solely by modulation of a single fractionating step in their biosynthesis.

Four conclusions arise from this analysis. First, more H is transmitted from water to fatty acids when growing on sugars than on acetate or succinate. This may reflect greater exchange of H associated with sugar isomerization reactions, and/or the fact that acetate feeds directly into fatty acid biosynthesis. Second, no H is transmitted from "chemoautotrophic" substrates to lipids, including formate, oxalate, and H_2. Third, the fractionations associated with different metabolic pathways are distinct but partially overlapping, in the order chemoautotrophy < photoautotrophy < heterotrophic growth on sugars < growth on TCA-cycle substrates. This pattern of changing fractionations mirrors the observed shifts in fatty acid δD values, and forms the basis for a plausible mechanistic link between lipid δD and metabolism. Fourth, the net lipid/water fractionation for a fatty acid is characteristic of a particular metabolism despite a wide possible range of δD values for potential organic substrates, because relatively little substrate H is incorporated into fatty acids. This means useful metabolic information can be extracted from the δD values of environmental lipids without the necessity of knowing or measuring δD values of precursor substrates.

Discussion

Our results demonstrate that 4 metabolically diverse *Proteobacteria* produce fatty acids with δD values that vary systematically

with the utilization of key metabolic pathways. The pattern is supported by previous culture studies of bacteria (19–21) and plants (11, 33) and is consistent with field observations. For example, fatty acids with odd carbon-numbered chains are substantially D-enriched (by up to 100‰) relative to those with even-numbered chains in marine POM (17). The former are attributed to heterotrophic bacteria, whereas the latter are likely the products of photosynthetic algae. Similar D enrichments of many bacterial fatty acids and all hopanols relative to their algal counterparts (i.e., even-numbered fatty acids and sterols) have also been observed in marine sediments (18). A 16:1 fatty acid with a δD value as low as −348‰ was detected in those sediments and is apparently generated in situ within the zone of maximal sulfate reduction. Its occurrence and isotopic composition are consistent with origins from chemoautotrophic sulfate-reducing bacteria (18). Studies of higher plants have shown several cases of D enrichment resulting from increased reliance on stored carbohydrates for growth and maintenance, and are consistent with a shift from photosynthesis to glycolysis as the primary metabolism (32, 34).

These similarities lead us to propose that the systematic variations reported here are a general feature resulting from the commonality of central metabolic pathways present in most microbes. Most of the same pathways are also present in higher life forms, although the resulting isotopic patterns will likely be complicated by compartmentalization and transport of lipids, metabolites, and water. Because we have sampled only a minute fraction of extant biota, further culture-based evidence is required to address these issues. In the mean time, confidence that we have observed a general phenomenon can be improved by understanding the mechanistic link between metabolism and D/H fractionation in lipids. Although we do not yet have sufficient data to prove such a link, we suggest that fractionations accompanying the reduction of $NADP^+$ provide a plausible—and perhaps unavoidable—mechanism. The basis for this hypothesis is summarized next.

Sources of D/H Variability in Fatty Acids. Isotopic labeling studies of fatty acid biosynthesis in vitro provide a rough accounting of the H sources for fatty acids (1, 35, 36). They indicate that the most important cellular H source is NAD(P)H, providing ≈50% of fatty acid H (Fig. S4). In most cases this comes solely from NADPH, but in some organisms such as *E. coli* it derives equally from both NADPH and NADH (22–24, 37). The methyl group of acetyl-CoA (25%) and water (25%) are of lesser importance. Four possible sources of isotopic variability in fatty acids can then be considered: (*i*) fractionations associated with substrate uptake and utilization; (*ii*) the isotopic composition of cellular water, acetate, and NADPH used for biosynthesis; (*iii*) variations in fractionation associated with reactions of the fatty acid biosynthetic pathway itself, including transfer of H from water and/or NADPH to fatty acids; and (*iv*) fractionations downstream from fatty acid biosynthesis such as desaturation and cellular transport.

Analysis of fractionation curves (see *Results*) removes *i* as a possibility. The lack of significant changes in fatty acid abundance and structure between culture conditions with very different lipid δD values rules out *iv*. Option *iii* is worth considering in some detail because multiple enzyme variants exist for 1 of the 2 reductive steps in fatty acid biosynthesis. β-ketoacyl ACP reductase transfers H from NADPH to odd-numbered carbon positions on the nascent fatty acid (step 4 in Fig. S4), whereas enoyl ACP reductase transfers H from either NADPH or NADH to even and odd positions (step 6 in Fig. S4) (22, 24). Only one type of β-ketoacyl ACP reductase (FabG) is known, but multiple variants (FabI, FabK, FabL) of enoyl reductase exist, sometimes in the same bacterium (23–25). Thus, differences in fractionations between flavin-free pyridine nucleotide-dependent enzymes like FabG and FabI versus flavoproteins like FabK might provide a mechanism for lipid D/H variability. The former catalyze direct hydride (H^-) transfer from NAD(P)H to fatty acids (24, 38, 39), whereas in the latter H^- is transferred via the flavin ring, which is susceptible to isotopic exchange with water (36, 40, 41). Differing fractionations between the enzyme types are therefore plausible. However, *E. coli* has only 1 of each reductase enzyme (i.e., a single FabG and FabI) yet lipid/water fractionations still vary substantially (23, 37, 42, 43). *C. necator* has several putative β-ketoacyl ACP reductases and FabI-type enoyl ACP reductases (26), but fractionations in *C. necator* are similar to those of *E. coli*. Thus, current data are inconsistent with fatty acid biosynthetic enzymes causing large variability in fatty acid δD values.

This leads us to consider option *ii*, the H-isotopic composition of water, acetate, and NAD(P)H, as sources for variability in fatty acid δD values. Variations in the D/H ratio of intracellular water have been observed in rapidly-growing *E. coli* and were attributed to the accumulation of water derived from the oxidation of organic substrates (44). Given that substrate δD values did not approach +200‰ or −300‰ in our study, and no systematic relationship between growth rate and fatty acid δD value was observed, the influence of varying intracellular water δD can be ruled out. We eliminate acetate as a source for isotopic variability on the following grounds. When *C. oxalaticus* grows on oxalate, it synthesizes acetate by converting oxalate to 3-phosphoglycerate (Box 3 in Fig. S5) (29). In contrast, 3-phosphoglycerate is generated by CO_2 fixation in the Calvin cycle when *C. oxalaticus* grows on formate (Box 7 in Fig. S5) (29). Thus, 2 very different modes of acetate synthesis (growth on oxalate vs. formate) yield similar fractionations, whereas synthesis of acetate by the same pathway of carbon fixation in different organisms (e.g., *C. oxalaticus* grown on formate and all higher plants) yields very different fractionations.

By process of elimination then, we arrive at the inference that the isotopic composition of NAD(P)H is likely responsible for observed variations in lipid/water fractionation. This conclusion is consistent both with the role of NAD(P)H as the major source of H in fatty acids, and with the ability of flavin-free reductases to transmit isotopic signals from NAD(P)H to fatty acids via hydride transfer reactions (38, 39). But why should the H-isotopic composition of NAD(P)H vary so greatly?

Isotopic Composition of NADPH. Biosynthetic reactions commonly require NADPH rather than NADH (27, 28, 45), thus we consider here only the cellular sources of NADPH for simplicity. Similar arguments apply to sources of NADH. In heterotrophic metabolism, the main sources of NADPH are the oxidative reactions catalyzed by glucose-6-phosphate dehydrogenase and 6-phosphogluconate dehydrogenase in the pentose phosphate pathway, isocitrate dehydrogenase and malic enzyme in the TCA cycle, and the NADH-NADPH converting transhydrogenase (Fig. S5) (28, 45). These oxidation reactions typically involve direct H^- transfer from substrate to $NADP^+$ (38, 39, 46, 47). Thus, the isotopic composition of each reduced NADPH will depend on that of the reaction substrate plus any isotope effects associated with the H^- transfer, and the total pool of NADPH will reflect the relative contributions of different pathways of energy metabolism. In oxygenic photoautotrophs, $NADP^+$ is reduced via the oxidation of water by ferredoxin-NADP oxidoreductase (48), providing yet another source of NADPH.

Isotope fractionations associated with many NADPH-generating reactions have been studied in vitro. Although their magnitudes vary greatly (up to 3,500‰, see Fig. S5) (49–52), it is not possible to confidently predict in vivo fractionations, and thus the isotopic composition of generated NADPH, from these data. In part this is because kinetic isotope effects will not be fully expressed as isotopic fractionations in committed pathways where the reactant is completely consumed (53). Nor can data from cultures be used, because even organisms grown on a single

substrate generate NADPH via multiple pathways (54). Nevertheless, it is reasonable to expect that the known variability in enzymatic isotope effects will manifest itself as varying δD values for NADPH generated by the respective pathways.

The enrichment of D in lipids from cultures grown on acetate and succinate is particularly interesting, because all of the relevant NADPH-generating reactions have normal isotope effects that should result in depletion of D. We consider 2 possible explanations here. First, D enrichments may arise during $NADP^+$ reduction in the TCA cycle. Both malic enzyme and isocitrate dehydrogenase generate NADPH via H^- transfer from an OH—C—H position (C-2 in isocitrate and malate). The expression of (normal) isotope effects in these reactions should be limited, because there is only one H available for abstraction. However, in both cases the substrate OH—C—H group is generated by the upstream removal of H from a corresponding methylene (H—C—H) position in the precursor molecule (succinate and citrate in Fig. S5). These upstream reactions are catalyzed by succinate dehydrogenase and aconitase. Both have been shown to express significant normal isotope effects (50, 52, 55), and are present in *C. necator* and *E. coli* (26, 43). For example, an average kinetic fractionation of 4,400‰ was measured for the removal of pro-*R* H from methylene groups in succinate by flavoprotein succinate dehydrogenase (55). The scale of this isotope effect is consistent with that expected for other flavoproteins, which have been proposed to break C—H bonds by H-tunneling mechanisms (56). These reactions should leave the remaining OH—C—H position very strongly enriched in D, a signal that can be transferred to NADPH. A second possible route to D enrichment of NADPH is through the action of transhydrogenases. These balance overproduction of NADPH due to high TCA cycle flux by converting it to NADH (54). Kinetic fractionations for transhydrogenases are typically large (800 to 3,500‰) (51), and should also leave the remaining NADPH strongly D-enriched.

The preceding discussion indicates that (*i*) NAD(P)H is the source for ≈50% of fatty acid hydrogen, (*ii*) the D/H ratios of NAD(P)H generated in different metabolic pathways probably vary over a large range, and (*iii*) those isotopic signals can be transmitted to fatty acids via hydride transfer reactions. Given these constraints, we should ask whether a link between metabolism and fatty acid δD values can in any way be avoided? Practically the only possibilities are if the relative fluxes of different NADPH-generating pathways remain constant, or if isotopic exchange homogenizes the NADPH pool with water. The former can be dismissed because metabolic flux studies in *E. coli* conclusively show that NADPH sources vary significantly during growth on different substrates (54, 57, 58).

The possibility of hydrogen exchange warrants further consideration because the relevant H position in NAD(P)H is moderately acidic. Experiments with D-labeled NADPH added to purified fatty acid biosynthetic enzymes in vitro showed complete conservation of the label in resultant fatty acids, whereas addition to crude cell extracts showed loss of the label (35). The latter result was attributed to isotope exchange via flavoproteins unrelated to lipid biosynthesis in the extract. If isotopic exchange of NADPH also occurs in vivo, it could serve to partially or entirely mute the fractionations accompanying NADPH production. As a concrete example, the slower growth rate of *R. palustris* might explain the smaller fractionations exhibited by this organism growing on acetate relative to *C. oxalaticus*. The extent to which this process is relevant in environmental samples is currently unknown, and must depend on turnover times for NADPH in growing cells. Although very little is known about the turnover of NADPH specifically, we note that the time scales for in vitro experiments (≈5 h) are quite long compared with typical turnover times for many common metabolic intermediates.

Conclusions

Existing culture and field data indicate that the D/H ratios of lipids vary substantially with growth conditions, and are systematically related to pathways of central metabolism. Organisms growing on heterotrophic substrates exhibit lipid/water fractionations ranging between approximately −150 to +200‰, photoautotrophic growth yields moderate D depletions (−150 to −250‰), whereas chemoautotrophic growth yields very strong D depletions of −200 to −400‰. We suggest that fractionations in the various pathways that reduce $NADP^+$ are the likely source of these variations. However, regardless of mechanism, such patterns hold enormous potential as biogeochemical tracers if they are shown to be widespread. This is particularly so given that the information provided by lipid δD values would be highly complementary to that encoded by molecular structure and C and N stable isotopes. Whereas ^{13}C largely records carbon fixation pathways in autotrophs, ^{2}H will respond to pathways of energy conservation. In heterotrophs, ^{13}C and ^{15}N generally reflect the history of substrate transfers through successive trophic levels, whereas ^{2}H could provide a snapshot of the metabolic pathways used for energy generation by individual organisms. The ability to connect lipids with energy metabolism could find numerous applications, from assessing the in situ metabolic lifestyle of facultative heterotrophs, to identifying modern and ancient communities based on chemoautotrophy, to apportioning the relative contributions of primary production and heterotrophic recycling to sedimentary organic matter.

Materials and Methods

For details, see *SI Methods*.

Culture Strains and Growth. *Cupriavidus oxalaticus* str. OX1, *Cupriavidus necator* str. H16, *Escherichia coli* K-12 str. MG1655, and *Rhodopseudomonas palustris* str. TIE-1 were grown in batch culture on a variety of substrates (Table 1). The δD of culture water was manipulated for *C. oxalaticus* and *E. coli* cultures by volumetrically diluting 99.9% purity D_2O with distilled deionized water. Substrate δD was not manipulated. Defined carbon sources were provided at 15 mM (except for 22.2 mM glucose in Ec5) for minimal media cultures of *Cupriavidus* and *E. coli*. Undefined carbon source LB was used for Ec6 cultures. *R. palustris* was cultivated in minimal medium with 20 mM thiosulfate for photoautotrophy and 20 mM acetate for both photoheterotrophy and aerobic heterotrophy. All media were 0.2-μm filter sterilized and inoculated with single colonies from rich media plates. Culture purity was checked by microscopy, colony morphology on plates, and—for *Cupriavidus*—the ability to grow on oxalate. Optical density (OD) at 600 nm (Cary 50 Bio, UV-Vis Spec) was used in conjunction with growth curve data (Fig. S1) to harvest cultures at a specific growth phase, generally mid-log phase. To harvest, ≈0.4 L was centrifuged for 20 min at 4,500 × *g*, yielding cell pellets ranging from 0.2 to 0.7 g of wet mass. These were stored at −20 °C before extraction.

Lipid Extraction and Quantification. Frozen cell pellets were lyophilized, then ≈20 mg of biomass was simultaneously transesterified and extracted in hexane/methanol/acetyl chloride at 100 °C for 10 min (59). The extract was concentrated under N_2 at room temperature. Fatty acid methyl esters (FAMEs) were analyzed by gas chromatography/mass spectrometry (GC/MS) on a Thermo-Scientific Trace/DSQ with a ZB-5ms column and PTV injector operated in splitless mode. Peaks were identified by comparison of mass spectra and retention times to authentic standards and library data. Relative abundances were calculated based on peak areas from the total ion chromatogram without further calibration. They are thus only semiquantitative, but still serve to demonstrate that fatty acid compositions did not change appreciably with growth substrate.

Isotopic Analyses. The δD values of the most abundant FAMEs were measured by GC/pyrolysis/isotope-ratio mass spectrometry (IRMS) on a Thermo-Scientific Delta$^+$XP. Chromatographic conditions were identical as for GC/MS analyses, and peaks were identified by retention order and relative height. Data are reported in the conventional δD notation versus the VSMOW standard, and are corrected for the addition of methyl H in the derivative. The root-mean-square (RMS) error of all external standards analyzed with these samples was 2.9‰. Typical precision (1σ) for replicate analyses of analytes was 3.4‰. The δD values of culture media, subsampled (1 mL) before inoculation, were measured on a Los Gatos Research

DLT-100 liquid water isotope analyzer. Samples were calibrated against 3 working standards with δD values ranging from −59 to +290‰. These were in turn calibrated against the VSMOW, GISP, and SLAP international standards (60). Average precision was 0.7‰ (1σ). δD values of nonexchangeable H in selected organic substrates were analyzed by Dr. A. Schimmelmann (Indiana University, Bloomington) by double-equilibration following the description in *SI Methods*.

ACKNOWLEDGMENTS. We thank A. Schimmelmann for substrate D/H analyses, M. Eek, and L. Zhang for assistance with lipid D/H analyses and J. Leadbetter and D. Newman and their respective research groups for providing insightful discussion and assistance with microbial cultures. This work was supported by National Science Foundation Grant EAR-0645502 (to A.L.S.) and a predoctoral fellowship (to X.Z.).

1. Robins RJ, et al. (2003) Measurement of ^{2}H distribution in natural products by quantitative ^{2}H NMR: An approach to understanding metabolism and enzyme mechanism? *Phytochem Rev* 2:87.
2. Billault I, Guiet S, Mabon F, Robins RJ (2001) Natural deuterium distribution in long-chain fatty acids is nonstatistical: A site-specific study by quantitative ^{2}H NMR spectroscopy. *ChemBioChem* 2:425–431.
3. Krull E, Sachse D, Mügler I, Thiele A, Gleixner G (2006) Compound-specific δ^{13}C and δ^2H analyses of plant and soil organic matter: A preliminary assessment of the effects of vegetation change on ecosystem hydrology. *Soil Biol Biochem* 38:3211–3221.
4. Pond KL, Huang Y, Wang Y, Kulpa CF (2002) Hydrogen isotopic composition of individual n-alkanes as an intrinsic tracer for bioremediation and source identification of petroleum contamination. *Environ Sci Technol* 36:724–728.
5. Sauer PE, Eglinton TI, Hayes JM, Schimmelmann A, Sessions AL (2001) Compound specific D/H ratios of lipid biomarkers from sediments as a proxy for environmental and climatic conditions. *Geochim Cosmochim Acta* 65:213–222.
6. Huang Y, Shuman B, Wang Y, Webb T (2002) Hydrogen isotope ratios of palmitic acid in lacustrine sediments record late Quaternary climate variations. *Geology* 30:1103–1106.
7. Sachse D, Radke J, Gleixner G (2004) Hydrogen isotope ratios of recent lacustrine sedimentary n-alkanes record modern climate variability. *Geochim Cosmochim Acta* 68:4877–4889.
8. Sessions AL, Sylva SP, Summons RE, Hayes JM (2004) Isotopic exchange of carbon-bound hydrogen over geologic timescales. *Geochim Cosmochim Acta* 68:1545–1559.
9. Sternberg L (1988) D/H ratios of environmental water recorded by D/H ratios of plant lipids. *Nature* 333:59–61.
10. Luo YH, Steinberg L, Suda S, Kumazawa S, Mitsui A (1991) Extremely low D/H ratios of photoproduced hydrogen by cyanobacteria. *Plant Cell Physiol* 32:897–900.
11. Yakir D, Deniro MJ (1990) Oxygen and hydrogen isotope fractionation during cellulose metabolism in Lemna gibba L. *Plant Physiol* 93:325–332.
12. Chikaraishi Y, Naraoka H, Poulson SR (2004) Hydrogen and carbon isotopic fractionations of lipid biosynthesis among terrestrial (C3, C4 and CAM) and aquatic plants. *Phytochemistry* 65:1369–1381.
13. Sessions AL, Burgoyne TW, Schimmelmann A, Hayes JM (1999) Fractionation of hydrogen isotopes in lipid biosynthesis. *Org Geochem* 30:1193–1200.
14. Chikaraishi Y, Naraoka H, Poulson SR (2004) Carbon and hydrogen isotopic fractionation during lipid biosynthesis in a higher plant (Cryptomeria japonica). *Phytochemistry* 65:323–330.
15. Chikaraishi Y, Suzuki Y, Naraoka H (2004) Hydrogen isotopic fractionations during desaturation and elongation associated with polyunsaturated fatty acid biosynthesis in marine macroalgae. *Phytochemistry* 65:2293–2300.
16. Zhang Z, Sachs JP (2007) Hydrogen isotope fractionation in freshwater algae: I. Variations among lipids and species. *Org Geochem* 38:582–608.
17. Jones A, Sessions AL, Campbell B, Li C, Valentine D (2008) D/H ratios of fatty acids from marine particulate organic matter in the California Borderland Basins. *Org Geochem* 39:485–500.
18. Li C, Sessions AL, Kinnaman FS, Valentine DL (2009) Hydrogen-isotopic variability in lipids from Santa Barbara Basin sediments. *Geochim Cosmochim Acta*, 10.1016/j.gca.2009.05.056.
19. Sessions AL, Jahnke LL, Schimmelmann A, Hayes JM (2002) Hydrogen isotope fractionation in lipids of the methane-oxidizing bacterium Methylococcus capsulatus. *Geochim Cosmochim Acta* 66:3955–3969.
20. Campbell BJ, Li C, Sessions AL, Valentine DL (2009) Hydrogen isotopic fractionation in lipid biosynthesis by H_2-consuming Desulfobacterium autotrophicum. *Geochim Cosmochim Acta* 73:2744–2757.
21. Valentine DL, Sessions AL, Tyler SC, Chidthaisong A (2004) Hydrogen isotope fractionation during H_2/CO_2 acetogenesis: Hydrogen utilization efficiency and the origin of lipid-bound hydrogen. *Geobiology* 2:179–188.
22. Marrakchi H, Zhang Y, Rock CO (2002) Mechanistic diversity and regulation of Type II fatty acid synthesis. *Biochem Soc Trans* 30:1050–1055.
23. Campbell JW, Cronan JE (2001) Bacterial fatty acid biosynthesis: Targets for antibacterial drug discovery. *Annu Rev Microbiol* 55:305–332.
24. White SW, Zheng J, Zhang Y, Rock CO (2005) The structural biology of Type II fatty acid biosynthesis. *Annu Rev Biochem* 74:791–831.
25. Rock CO, Jackowski S (2002) Forty years of bacterial fatty acid synthesis. *Biochem Biophys Res Commun* 292:1155–1166.
26. Pohlmann A, et al. (2006) Genome sequence of the bioplastic-producing ''Knallgas'' bacterium Ralstonia eutropha H16. *Nat Biotechnol* 24:1257–1262.
27. Gottschalk G (1986) *Bacterial Metabolism* (Springer, New York).
28. White D (2000) *The physiology and biochemistry of prokaryotes* (Oxford Univ Press, New York).
29. Quayle JR (1961) Metabolism of C1 compounds in autotrophic and heterotrophic microorganisms. *Annu Rev Microbiol* 15:119–152.
30. Friedrich CG, Bowien B, Friedrich B (1979) Formate and oxalate metabolism in Alcaligenes eutrophus. *J Gen Microbiol* 115:185–192.
31. Sessions AL, Hayes JM (2005) Calculation of hydrogen isotopic fractionations in biogeochemical systems. *Geochim Cosmochim Acta* 69:593–597.
32. Yakir D (1992) Variations in the natural abundance of oxygen-18 and deuterium in plant carbohydrates. *Plant Cell Environ* 15:1005–1020.
33. Luo YH, Sternberg L (1991) Deuterium heterogeneity in starch and cellulose nitrate of CAM and C_3 plants. *Phytochemistry* 30:1095–1098.
34. Sessions AL (2006) Seasonal changes in D/H fractionation accompanying lipid biosynthesis in Spartina alterniflora. *Geochim Cosmochim Acta* 70:2153–2162.
35. Saito K, Kawaguchi A, Okuda S, Seyama Y, Yamakawa T (1980) Incorporation of hydrogen atoms from deuterated water and stereospecifically deuterium-labeled nicotinamide nucleotides into fatty acids with the Escherichia coli fatty acid synthetase system. *Biochim Biophys Acta* 618:202–213.
36. Schmidt HL, Werner RA, Eisenreich W (2003) Systematics of ^{2}H patterns in natural compounds and its importance for the elucidation of biosynthetic pathways. *Phytochem Rev* 2:61–85.
37. Heath RJ, Rock CO (1995) Enoyl-acyl carrier protein reductase (fabI) plays a determinant role in completing cycles of fatty acid elongation in Escherichia coli. *J Biol Chem* 270:26538–26542.
38. Popjak G (1970) in *The Enzymes*, ed Boyer PD (Academic, New York), pp 115–215.
39. McMurry JE, Begley TP (2005) *The Organic Chemistry of Biological Pathways* (Roberts and Company, Englewood, NJ).
40. Simon H, Kraus A (1976) in *Isotopes in Organic Chemistry*, eds Buncel E, Lee CC (Elsevier Science, Amsterdam), pp 153–229.
41. Ghisla S, Massey V (1989) Mechanisms of flavoprotein catalyzed reactions. *Eur J Biochem* 181:1–17.
42. Bergler H, Fuchsbichler S, Högenauer G, Turnowsky F (1996) The enoyl-[acyl-carrier-protein] reductase (FabI) of Escherichia coli, which catalyzes a key regulatory step in fatty acid biosynthesis, accepts NADH and NADPH as cofactors and is inhibited by palmitoyl-CoA. *Eur J Biochem* 242:689–694.
43. Riley M, et al. (2006) Escherichia coli K-12: A cooperatively developed annotation snapshot-2005. *Nucleic Acids Res* 34:1–9.
44. Kreuzer-Martin HW, Lott MJ, Ehleringer JR, Hegg EL (2006) Metabolic processes account for the majority of the intracellular water in log-phase Escherichia coli cells as revealed by hydrogen isotopes. *Biochemistry* 45:13622–13630.
45. Ingraham JL, Maaløe O, Neidhardt FC (1983) *Growth of the Bacterial Cell* (Sinauer, Sunderland, MA).
46. Edens WA, Urbauer JL, Cleland WW (1997) Determination of the chemical mechanism of malic enzyme by isotope effects. *Biochemistry* 36:1141–1147.
47. Jackson J (2003) Proton translocation by transhydrogenase. *FEBS Lett* 545:18–24.
48. Shin M (2004) How is ferredoxin-NADP reductase involved in the NADP photoreduction of chloroplasts? *Photosynth Res* 80:307–313.
49. O'Leary MH (1989) Multiple isotope effects on enzyme-catalyzed reactions. *Annu Rev Biochem* 59:377–401.
50. Thomson JF, Nance SL, Bush KJ, Szczepanik PA (1966) Isotope and solvent effects of deuterium on aconitase. *Arch Biochem Biophys* 117:65–74.
51. Jackson JB, Peake SJ, White SA (1999) Structure and mechanism of proton-translocating transhydrogenase. *FEBS Lett* 464:1–8.
52. Lenz H, et al. (1971) Stereochemistry of si-citrate synthase and ATP-citrate-lyase reactions. *Eur J Biochem* 24:207–215.
53. Hayes JM (2001) Fractionation of carbon and hydrogen isotopes in biosynthetic processes. *Rev Mineral Geochem* 43:225–277.
54. Sauer U, Canonaco F, Heri S, Perrenoud A, Fischer E (2004) The soluble and membrane-bound transhydrogenases UdhA and PntAB have divergent functions in NADPH metabolism of Escherichia coli. *J Biol Chem* 279:6613–6619.
55. Retey J, et al. (1970) Stereochemical studies of the exchange and abstraction of succinate hydrogen on succinate dehydrogenase. *Eur J Biochem* 14:232–242.
56. Nesheim JC, Lipscomb JD (1996) Large kinetic isotope effects in methane oxidation catalyzed by methane monooxygenase: Evidence for C—H bond cleavage in a reaction cycle intermediate. *Biochem* 35:10240–10247.
57. Zhao J, Baba T, Mori H, Shimizu K (2004) Effect of zwf gene knockout on the metabolism of Escherichia coli grown on glucose or acetate. *Metab Eng* 6:164–174.
58. Zhao J, Shimizu K (2003) Metabolic flux analysis of Escherichia coli K12 grown on ^{13}C-labeled acetate and glucose using GC-MS and powerful flux calculation method. *J Biotechnol* 101:101–117.
59. Rodríguez-Ruiz J, Belarbi E, Sánchez JLG, Alonso DL (1998) Rapid simultaneous lipid extraction and transesterification for fatty acid analyses. *Biotechnol Tech* 12:689–691.
60. Coplen TB (1988) Normalization of oxygen and hydrogen isotope data. *Chem Geol* 72:293–297.
61. Chikaraishi Y (2003) Compound-specific δD–δ^{13}C analyses of n-alkanes extracted from terrestrial and aquatic plants. *Phytochemistry* 63:361–371.

Isotopic remembrance of metabolism past

David L. Valentine[1]

Department of Earth Science and Marine Science Institute, University of California, Santa Barbara, CA 93106

At the interface of Earth science, chemistry, and biology, scientists are working to interpret the record of biological markers, or biomarkers, retained in natural environments. Although these molecular fossils take many forms, arguably the most useful and durable have lipid character and are amenable to gas-chromatographic separation. Many such compounds are related to extant natural products by distinctive molecular structures and thus can be related to specific taxonomic groups, functions, or processes. Moreover, biomarkers may contain information in their relative abundance of light and heavy isotopes. The isotopes of carbon have been most fully explored (1), but following a decade of advances in compound-specific deuterium analysis (2, 3), the relative abundance of the hydrogen isotopes protium (^{1}H) and deuterium (^{2}H or D) has received increasing attention. Most commonly these analyses are used to track past changes of climate and aridity, enabled by the strong correlation of deuterium content between plant-derived lipids and source water (4–8). In this issue of PNAS, Zhang et al. (9) move in a new direction and lay the groundwork for a proxy of cellular metabolism based on lipid deuterium. They present results from laboratory experiments with bacterial cultures demonstrating that the deuterium content of lipid biomarker compounds is strongly modulated by the central biochemical pathway a cell uses to generate reducing power for biosynthesis. These results suggest that the deuterium content of lipid biomarkers in the geomolecular record may provide a window into the central metabolic pathways active at a given time and place—isotopic remembrance of metabolism past.

The cast of bacterial characters examined by Zhang et al. (9) includes four strains representing three lineages known as α, β, and γ Proteobacteria. The heterotroph *Escherichia coli*, a γ-proteobacterium, is the most (in)famous and was cultivated with oxygen on organic substrates. The phototroph *Rhodopseudomonas palustris* is an α-proteobacterium capable of both phototrophic and heterotrophic growth; it was cultivated both in the light, without oxygen and with or without organic compounds, and as a respiratory heterotroph, with oxygen and organic compounds. Finally, two species from the β-proteobacterial genus *Cupriavidus*—*C. necator* and *C. oxalaticus*—were cultivated under respiratory conditions as heterotrophs, as well as under an unusual condition where energy is derived from simple carbon-containing compounds, but biomass is derived from carbon dioxide autotrophy and water hydrotrophy. (I define hydrotrophy with respect to the sources of cellular hydrogen: in hydrotrophic metabolism, all carbon-bound cellular hydrogen derives from water.) The growth substrates for these different bacteria represent entry points into different metabolic cycles: the Embden–Meyerhof, Entner–Doudoroff, and pentose phosphate pathways, fed by sugars; the tricarboxylic acid (TCA) cycle, fed by organic acids; and autotrophic/hydrotrophic growth, fed both by small molecules such as formate and oxalate and by light energy. Zhang et al. systematically varied the deuterium content of the water in the growth medium while holding the deuterium content of

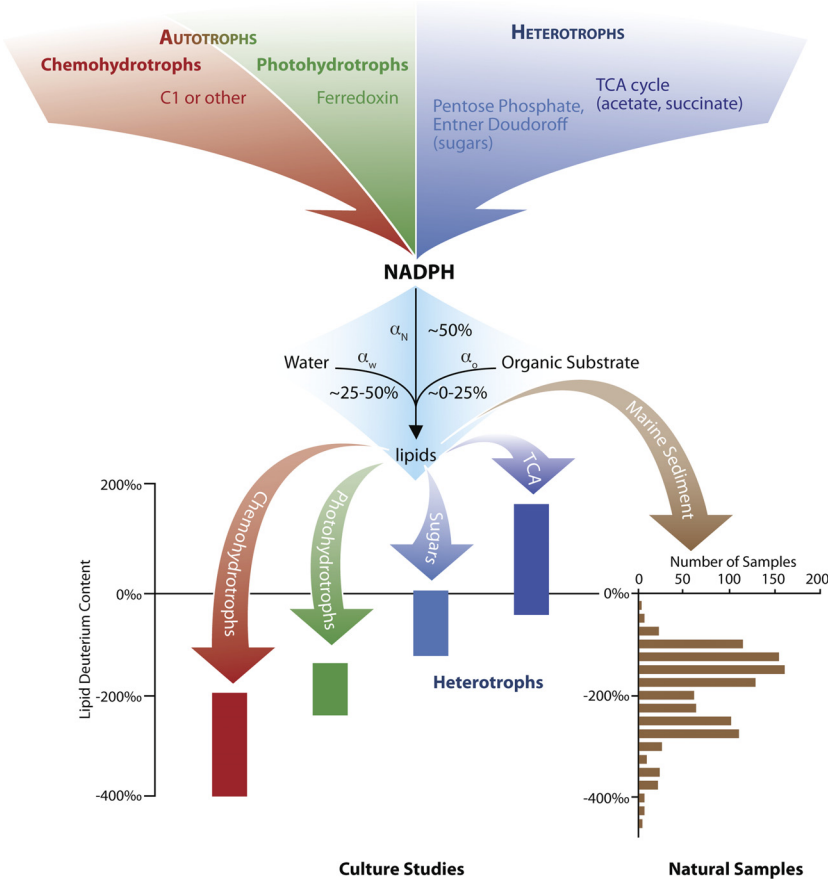

Fig. 1. At the top: NADPH is the primary immediate biosynthetic precursor of hydrogen for lipids and is generated by diverse mechanisms associated with different central metabolic pathways as indicated. In the middle: The deuterium content of lipids is set by the balance of hydrogen precursors, namely water, NADPH, and organic material. The approximate percentage contribution of each source is indicated. Each reaction is accompanied by a fractionation, designated by α. The results of Zhang et al. (9) indicate that fractionation associated with lipid biosynthesis is secondary to the upstream reactions that set the deuterium content of NADPH. At the bottom: The deuterium content of lipid biomarkers is displayed, all originating from waters with similar deuterium content. At left are the fatty acids from the cultivation studies of Zhang et al., distinguished by substrates that feed into the identified metabolic pathways. At right is a histogram summarizing the distribution of deuterium content for ≈1,000 analytes extracted from the anoxic marine sediments of the Santa Barbara Basin (11). Included in the histogram are several classes of compounds, including fatty acids, alcohols, alkanes, and isoprenoids, the latter of which tend to be depleted in deuterium. Fatty acids from this sediment range in deuterium content from −32‰ to −280‰, consistent with distinct contributions from different metabolic pathways.

Author contributions: D.L.V. wrote the paper.

The author declares no conflict of interest.

See companion article on page 12580.

[1]E-mail: valentine@geol.ucsb.edu.

organic substrates constant. They then measured the extent of deuterium fractionation in the cells' lipids. This experimental design mathematically constrains the sources providing hydrogen to lipids for each growth substrate, and it enables graphic representation of the isotopic relationships through fractionation curves (9, 10). With the aid of these curves the authors rigorously exclude lipid biosynthetic reactions as a major determinant of the observed deuterium fractionation.

To explore the source of the observed fractionation the authors look to the enormous variation in lipid deuterium content within each single strain when grown on different substrates—as much as 50% (500‰ in the nomenclature used by geochemists; for perspective, the deuterium content of most plants varies by only ≈one-tenth this much). Given that lipid biosynthetic reactions are not responsible for this variation, the authors surmise that these dramatic differences must arise from differences in the deuterium content of the primary molecular precursor to lipid hydrogen, namely the reduced form of nicotinamide adenine dinucleotide phosphate, NADPH. The hydrogen of NADPH is derived from different reactions in the various metabolic pathways but is central to lipid biosynthesis, as shown schematically in Fig. 1. Hydride transferred from NADPH to lipids seemingly carries a deuterium signature set by its metabolic history.

These results fundamentally change our understanding as to how lipid deuterium content is set. It is well established that lipid deuterium content is controlled at the first order by deuterium levels in potential sources—namely water and/or organic molecules (10). In the absence of evidence to the contrary, the paradigm has been that isotopic fractionation during lipid biosynthesis is superimposed on these sources to set the ultimate deuterium content of the lipid. Such fractionation, commonly designated by the factor α, seemingly discriminates against deuterium. (This aspect of lipid biosynthesis is highlighted within the shaded region in the center of Fig. 1.) Zhang et al. (9) overturn this paradigm by demonstrating that the upstream metabolic pathways generating reducing power for lipid biosynthesis exert greater control on ultimate lipid deuterium content than does net fractionation during biosynthesis. Water and organic material do supply the deuterium in lipids, but the pathway that generates biosynthetic reducing power in the form of NADPH serves as an important second level of control. Fractionation during lipid biosynthesis likely impacts lipid deuterium content too, but it now appears relegated to a tertiary role.

Through a comparative analysis of the four strains identified above and previous studies with other organisms, Zhang et al. (9) provide further correlative evidence that lipids derived through the same pathways, but in different organisms, share similar deuterium content. Perhaps more fortuitously, different pathways yield different (although slightly overlapping) deuterium contents. These trends are highlighted in Fig. 1, with four metabolic types being differentiated by the resulting lipid deuterium content. When corrected for the deuterium content of source water, cultivation studies yield lipid deuterium contents ranging over ≈600‰. These differences point toward the potential application of lipid deuterium as an indicator of central metabolic pathways. But is such variability mirrored in the environment?

A recent study by Li et al. (11) helps to address this question through analysis of deuterium content in more than 1,100 lipids of putative marine origin from the sediments of the Santa Barbara Basin. A histogram summarizing their results is presented in Fig. 1, demonstrating an overall range of ≈500‰ for lipid deuterium, with a range of ≈250‰ for fatty acids. This broad range and the underlying patterns are promising and are consistent with the geomolecular record of lipid deuterium containing information about metabolism. But how might we extract and interpret this information?

Numerous questions need to be more fully addressed before the results of Zhang et al. (9) can be broadly applied to nature and the geologic record: Do all organisms follow similar metabolic patterns of deuterium abundance, or more realistically, are the inevitable exceptions acceptable? Where will the lipids of fermentative organisms lie on the deuterium scale? How does natural variability in growth, environmental conditions, and lipid biosynthesis impact lipid deuterium content? For how long will the information be retained in the geologic record? What specific molecules serve as the most promising targets? Can contributions from multiple sources be deconvoluted to estimate deuterium content of individual organisms? Do patterns observed for fatty acids apply to other biomarkers? Clearly there is much work still to be done, but the results of Zhang et al. point in an exciting direction. Support and interest willing, an approach that simultaneously investigates deuterium systematics in both modern and geologic systems holds promise. Three basic avenues of inquiry are necessary, and indeed underway. First, measurement of deuterium content and fractionation for lipid biomarkers is needed for a variety of other organisms and metabolic types to determine the applicability and limitations of the present results. Second is investigating modern environmental systems in which the deuterium content and distribution of lipid biomarkers can be compared with extant metabolism. Third, the geologic record should be mined for patterns and variations in deuterium content of lipid biomarkers, with an eye toward assessing preservation beyond a few million years (12) and extracting primary signals. After such validation activities, then maybe a new paleometabolic proxy will be born.

Beyond the development of a new paleometabolic proxy, the present results may find application for interpreting paleoclimatic and environmental lipid deuterium results, as well as in studies of metabolic dynamics. Environmental changes such as temperature, salinity, or incident radiation may subtly impact the dynamics of NADPH in the cell and thereby affect resulting lipid deuterium content. Such a mechanism should be considered as a possible explanation for the minor variations observed in numerous studies. The use of deuterium variations in other metabolic products might even allow us to track the flow of reducing power; simple measurements might yield insight into the underlying metabolic dynamics, with application toward fermentations, natural product biosynthesis, inhibition studies, and other metabolic flux investigations.

1. Hayes JM (2001) Fractionation of carbon and hydrogen isotopes in biosynthetic processes. *Stable Isotope Geochemistry,* Reviews in Mineralogy and Geochemistry (Mineralogical Soc America, Washington, DC), Vol 43, pp 225–277.
2. Sessions AL (2006) Isotope-ratio detection for gas chromatography. *J Sep Sci* 29:1946–1961.
3. Sessions AL, Burgoyne TW, Schimmelmann A, Hayes JM (1999) Fractionation of hydrogen isotopes in lipid biosynthesis. *Org Geochem* 30:1193–1200.
4. Chikaraishi Y, Naraoka H (2003) Compound-specific delta D-delta C-13 analyses of n-alkanes extracted from terrestrial and aquatic plants. *Phytochemistry* 63:361–371.
5. Huang YS, Shuman B, Wang Y, Webb T (2002) Hydrogen isotope ratios of palmitic acid in lacustrine sediments record late Quaternary climate variations. *Geology* 30:1103–1106.
6. Sachse D, Radke J, Gleixner G (2004) Hydrogen isotope ratios of recent lacustrine sedimentary n-alkanes record modern climate variability. *Geochim Cosmochim Acta* 68:4877–4889.
7. Sauer PE, Eglinton TI, Hayes JM, Schimmelmann A, Sessions AL (2001) Compound-specific D/H ratios of lipid biomarkers from sediments as a proxy for environmental and climatic conditions. *Geochim Cosmochim Acta* 65:213–222.
8. Sternberg LDL (1988) D/H ratios of environmental water recorded by D/H ratios of plant lipids. *Nature* 333:59–61.
9. Zhang X, Gillespie A, Sessions AL (2009) Large D/H variations in bacterial lipids reflect central metabolic pathways. *Proc Natl Acad Sci USA* 106:12580–12586.
10. Sessions AL, Hayes JM (2005) Calculation of hydrogen isotopic fractionations in biogeochemical systems. *Geochim Cosmochim Acta* 69:593–597.
11. Li C, Sessions AL, Kinnaman FS, Valentine DL (2009) Hydrogen-isotopic variability in lipids from Santa Barbara Basin sediments. *Geochim Cosmochim Acta*, 10.1016/j.gca.2009.05.056.
12. Sessions AL, Sylva SP, Summons RE, Hayes JM (2004) Isotopic exchange of carbon-bound hydrogen over geologic time scales. *Geochim Cosmochim Acta* 68:1545–1559.

Supporting Information

Zhang et al. 10.1073/pnas.0903030106

SI Methods

Culture Media and Growth Conditions. *Cupriavidus oxalaticus* str. OX1 (DSM 1105^T) and *Cupriavidus necator* str. H16 (previously known as *Ralstonia eutropha*, DSM 428) were cultivated in minimal medium described by Dijkhuizen and Harder (1). We used 15 mM rather than 20 mM phosphate buffering (pH 7.2) for pH control. *Escherichia coli* K-12 str. MG1655 was cultivated in M9 minimal media (2). Glucose (22.2 mM) was replaced with other carbon sources at 15 mM for the appropriate experiments (see Table 1). All minimal media cultures were amended with EDTA-chelated trace elements formulated according to Flagan et al. (3). *Rhodopseudomonas palustris* str. TIE-1 was cultivated in freshwater minimal medium (4) according to Rashby et al. (5) containing 20 mM bicarbonate buffer and 20 mM thiosulfate for photoautotrophic growth, 20 mM N-Tris(hydroxymethyl)methyl-2-aminoethanesulfonic acid buffer and 20 mM acetate for photoheterotrophic growth, and 20 mM acetate for aerobic heterotrophic growth. Growth substrates were potassium oxalate monohydrate (Sigma), sodium formate (Mallinckrodt), anhydrous D-glucose (Mallinckrodt), anhydrous sodium acetate (Sigma), sodium succinate hexahydrate (≥ 99%, Sigma), sodium pyruvate (≥ 99%, Sigma), D-(−)-fructose (≥ 99%, Sigma), and sodium D-gluconate (97%, Sigma). Aerobic cultures (0.5 L) of *C. oxalaticus*, *C. necator*, and *E. coli* were grown shaking at 200 or 250 rpm in 1-L combusted Pyrex flasks. *Cupriavidus* was cultivated at 30 °C, *E. coli* at 37 °C. Phototrophic cultures of *R. palustris* were incubated in 2-L flasks with 1 L of N_2 headspace and 2,000-lux illumination at room temperature. Aerobic heterotrophic cultures (1 L) were grown at 30 °C, shaking at 250 rpm in the dark.

Isotopic Analyses. The δD values of the most abundant FAMEs were measured on a ThermoScientific GC coupled to a Delta$^+$XP isotope-ratio mass spectrometer (IRMS) via the GC/TC pyrolysis interface. Chromatographic conditions were identical as for GC/MS analysis, and peaks were identified by retention order and relative height. The H_3-factor was calibrated daily using multiple peaks of H_2 reference gas at varying intensity, and was stable at ≈4.7–4.8 ppm/mV. Data are reported in the conventional δD notation versus the VSMOW standard, and are corrected for the addition of methyl H in the derivative. The δD value of added methyl H used for this correction was determined by analyzing the dimethyl derivative of phthalic acid for which the δD value of ring H is known. Replicate analyses were performed for all samples except Co1-Co4, and an external standard containing either 16 *n*-alkanes (*R. palustris* and *E. coli* data) or 8 FAMEs (*Cupriavidus* data) of known δD value was analyzed every 5th injection. The root-mean-square (RMS) error of all external standards analyzed with these samples was 2.9‰. Typical precision (1σ) based on multiple analyses of analytes was 3.4‰. The δD of culture media was measured on a Los Gatos Research DLT-100 liquid water isotope analyzer. This instrument measures by absorption spectroscopy, and has been evaluated in detail by Lis et al. (6). Six sequential aliquots (0.8 μL of each) of each sample were injected, with the first 3 discarded, to minimize memory effects.

Substrate δD values were measured by equilibrating selected aliquots with at least 2 waters of differing D/H ratio (as steam) to control for the presence of exchangeable H before conversion to H_2 by sequential combustion/reduction (7) and analysis by dual-inlet IRMS. The isotope ratio of nonexchangeable H was then calculated by mass balance from the 2 exchanged samples (8). Because of significant uncertainties associated with this correction, uncertainties in reported values may be as high as ± 20‰. Gluconate was also analyzed by this method, but did not yield reliable results for unknown reasons. The extreme D enrichment of formate indicated by this method is similar to that obtained for a separate formate sample, from a different supplier, measured by a different lab using a different analytical method (9) and is considered reliable.

1. Dijkhuizen L, Harder W (1975) Substrate inhibition in Pseudomonas oxalaticus OX1: A kinetic study of growth inhibition by oxalate and formate using extended cultures. *Antonie van Leeuwenhoek* 41:135–146.
2. Sambrook J, Fritsch EF, Maniatis T (1989) *Molecular Cloning: A Laboratory Manual* (Cold Spring Harbor Laboratory, Plainview, NY).
3. Flagan S, Ching WK, Leadbetter JR (2003) Arthrobacter strain VAI-A utilizes acyl-homoserine lactone inactivation products and stimulates quorum signal biodegradation by Variovorax paradoxus. *Appl Environ Microbiol* 69:909–916.
4. Ehrenreich A, Widdel F (1994) Anaerobic oxidation of ferrous iron by purple bacteria, a new type of phototrophic metabolism. *Appl Environ Microbiol* 60:4517–4526.
5. Rashby SE, Sessions AL, Summons RE, Newman DK (2007) Biosynthesis of 2-methylbacteriohopanepolyols by an anoxygenic phototroph. *Proc Natl Acad Sci USA* 104:15099.
6. Lis G, Wassenaar LI, Hendry MJ (2008) High-precision laser spectroscopy D/H and $^{18}O/^{16}O$ measurements of microliter natural water samples. *Anal Chem* 80:287–293.
7. Schimmelmann A, DeNiro M (1993) Preparation of organic and water hydrogen for stable isotope analysis: Effects due to reaction vessels and zinc reagent. *Anal Chem* 65:789–792.
8. Schimmelmann A (1991) Determination of the concentration and stable isotopic composition of nonexchangeable hydrogen in organic matter. *Anal Chem* 63:2456–2459.
9. Campbell BJ, Li C, Sessions AL, Valentine DL (2009) Hydrogen isotopic fractionation in lipid biosynthesis by H_2-consuming Desulfobacterium autotrophicum. *Geochim Cosmochim Acta* 73:2744–2757.

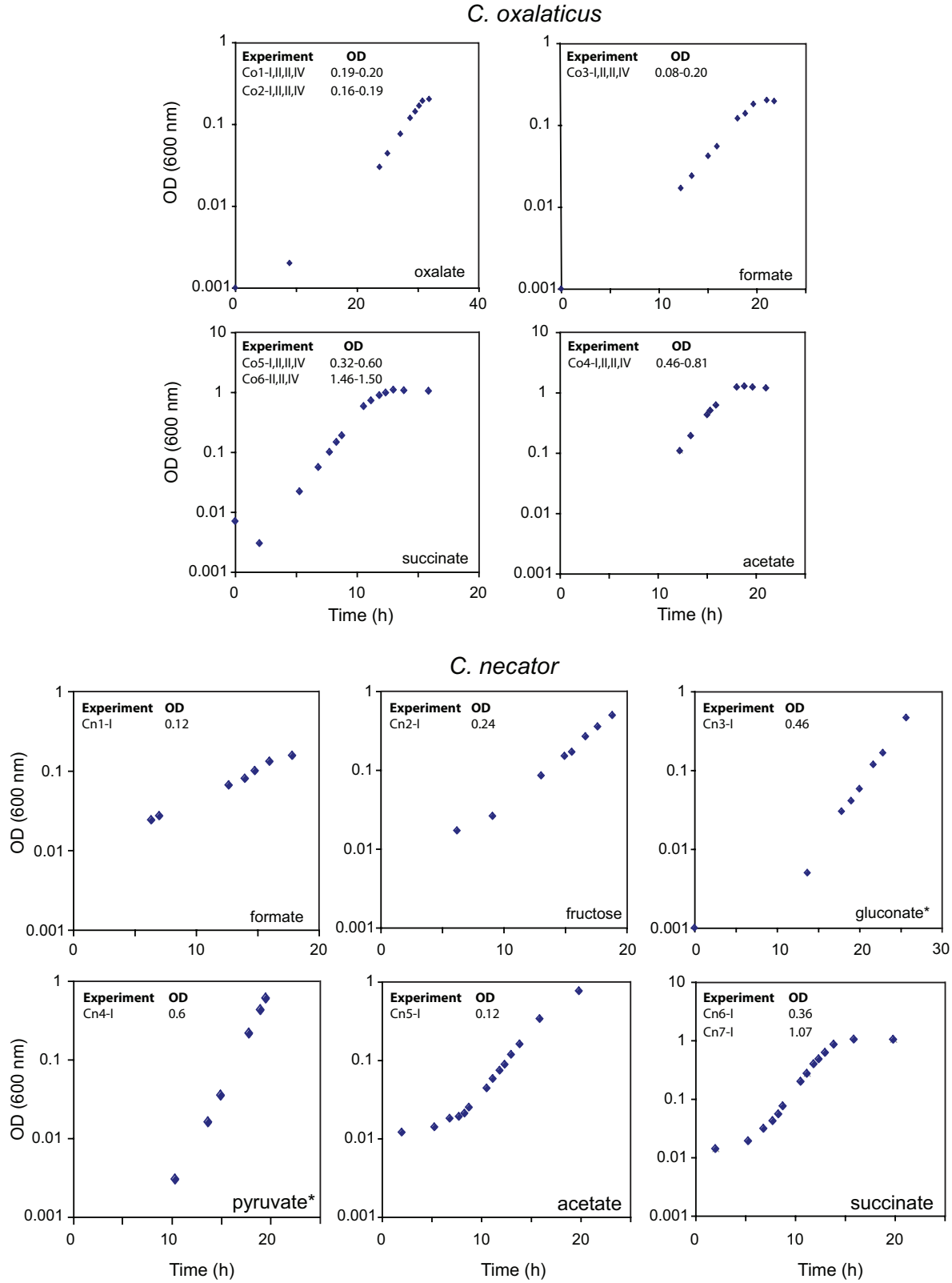

Fig. S1. Representative growth curves for *C. oxalaticus*, *C. necator*, *E. coli*, and *R. palustris* cultures on selected substrates. OD_{600nm} values at harvest are listed. For most substrates, plotted growth data are from a single culture grown to stationary phase to define the growth curve, but not then analyzed. Panels containing substrates marked with asterisks show the growth curve from a culture that was harvested for isotopic analysis, generally in mid-log phase.

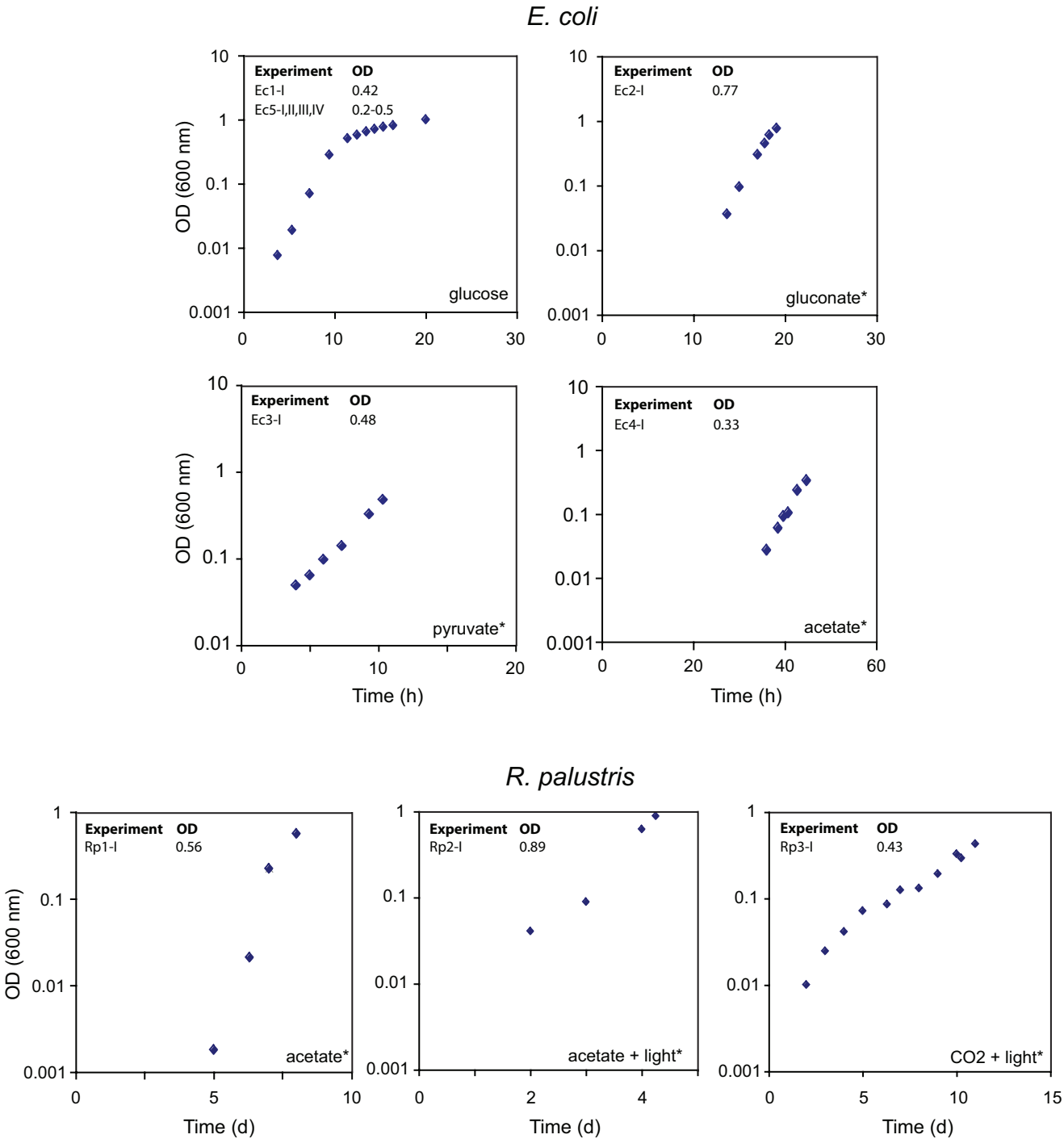

Fig. S1. continued.

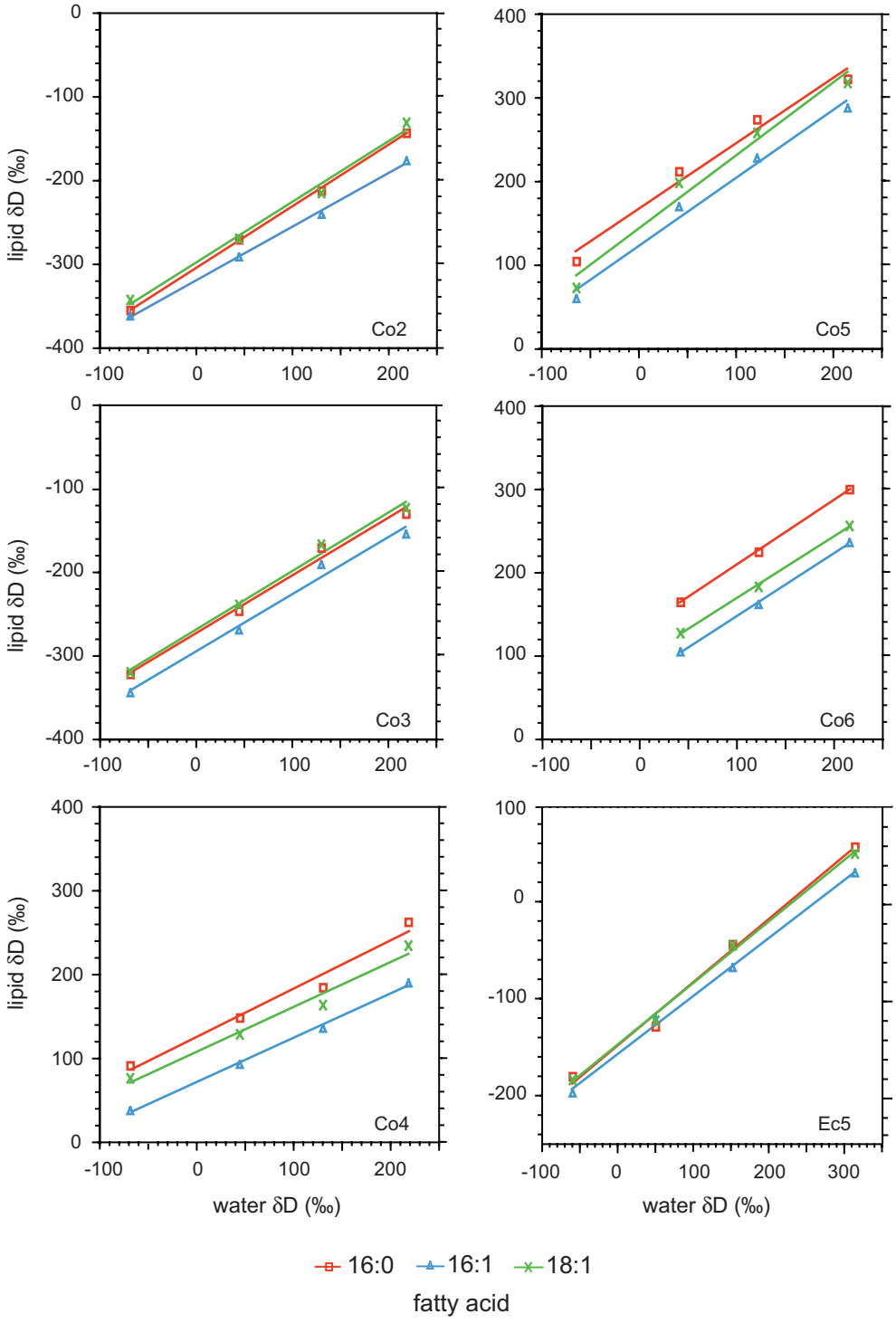

Fig. S2. Relationship between fatty acid and water δD values for *C. oxalaticus* and *E. coli* cultures. The slope of each regression curve is equivalent to $X_w\alpha_{l/w}$. Culture numbers are labeled in the lower right of each plot.

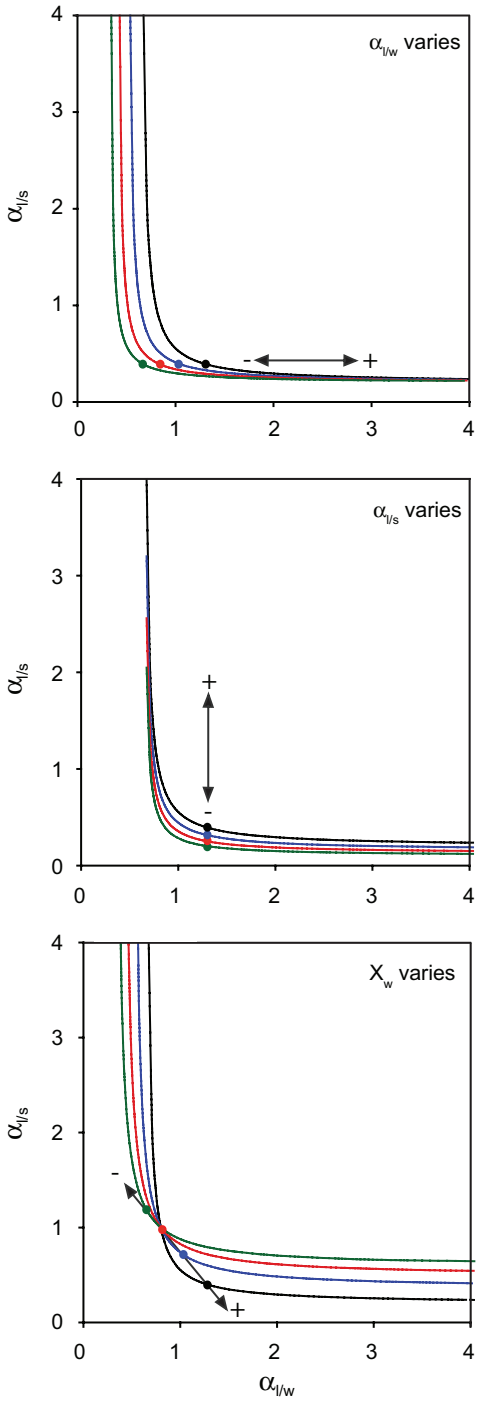

Fig. S3. Fractionation curves for hypothetical sets of cultures that differ only in a single parameter ($\alpha_{l/s}$, $\alpha_{l/w}$, or X_w). The plotted curves reflect 20% incremental changes in the specified parameter and arrows indicate the direction of change for an entire curve. The effects can be treated as independent, such that the result of changing 2 parameters can be estimated by vector addition. Filled circles mark $X_w = 0.5$. To account for curves that shift up and to the right (e.g., those in Fig. 3), both $\alpha_{l/s}$ and $\alpha_{l/s}$ must simultaneously change.

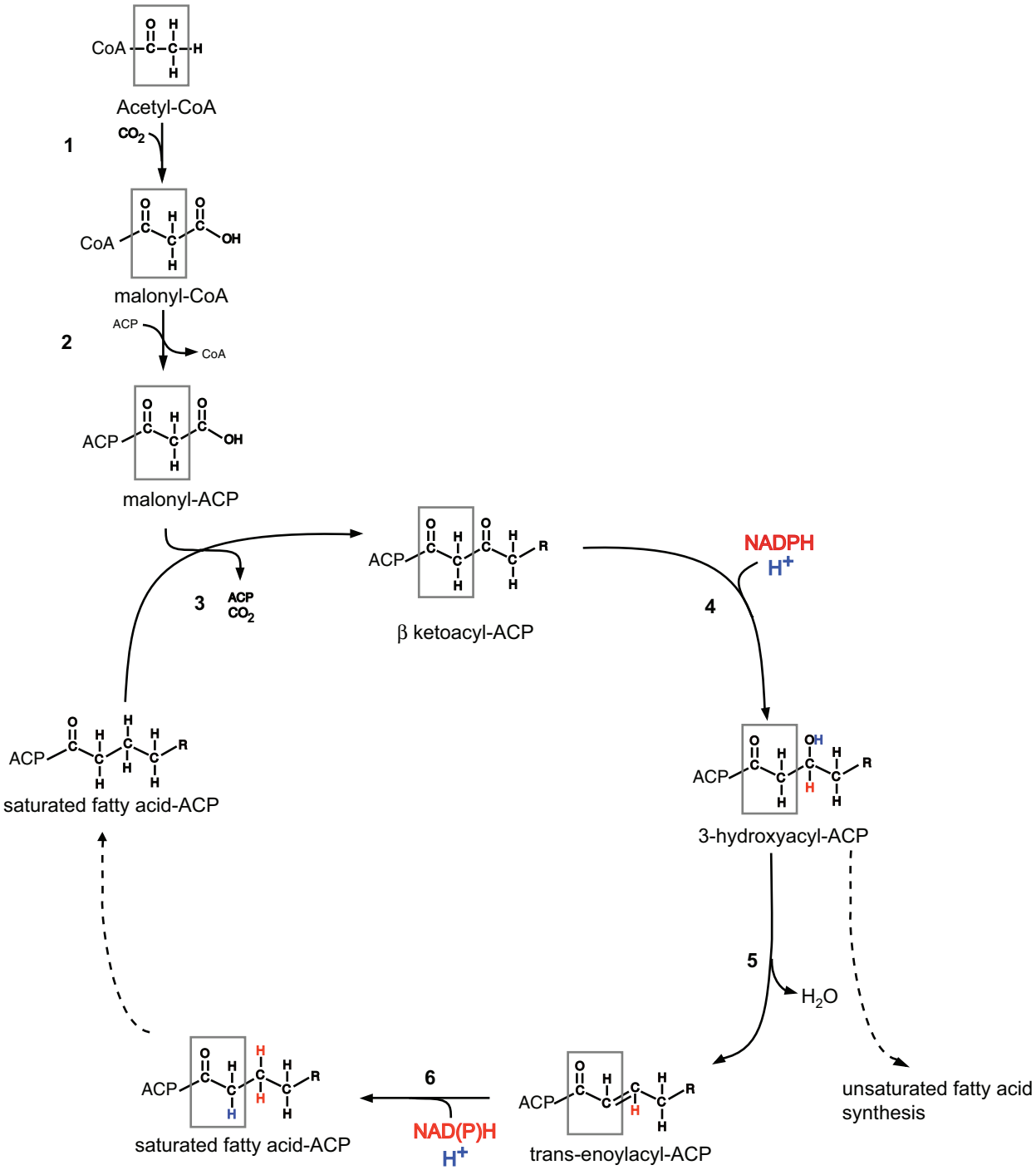

Fig. S4. Fatty acid biosynthetic pathway highlighting cellular sources of H (refs. 1–5). (1) Acetyl-CoA carboxylase, which is regulated to control carbon flux into lipids. (2) Malonyl CoA-ACP transacylase. (3) β-ketoacyl ACP synthase (FabB, FabF, FabH). FabH controls biosynthesis initiation and fatty acid composition based on acyl-CoA specificity, whereas FabB and FabF catalyze subsequent rounds of elongation by condensing malonyl-ACP with acyl-ACP. (4) β-ketoacyl ACP reductase (FabG). (5) β-hydroxyacyl ACP dehydratase (FabZ, FabA). (6) Enoyl ACP reductase (FabI, FabK, FabL).

1. Marrakchi H, Zhang Y, Rock CO (2002) Mechanistic diversity and regulation of Type II fatty acid synthesis. *Biochem Soc Trans* 30:1050–1055.
2. Magnuson K, Jackowski S, Rock CO, Cronan JE (1993) Regulation of fatty acid biosynthesis in Escherichia coli. *Microbiol Molec Biol Rev* 57:522–542.
3. Campbell JW, Cronan JE (2001) Bacterial fatty acid biosynthesis: Targets for antibacterial drug discovery. *Annu Rev Microbiol* 55:305–332.
4. Rock CO, Cronan JE (1996) Escherichia coli as a model for the regulation of dissociable (type II) fatty acid biosynthesis. *Biochim Biophys Acta* 1302:1–16.
5. White S, Zheng J, Zhang Y, Rock CO (2005) The structural biology of Type II fatty acid biosynthesis. *Annu Rev Biochem* 74:791–831.

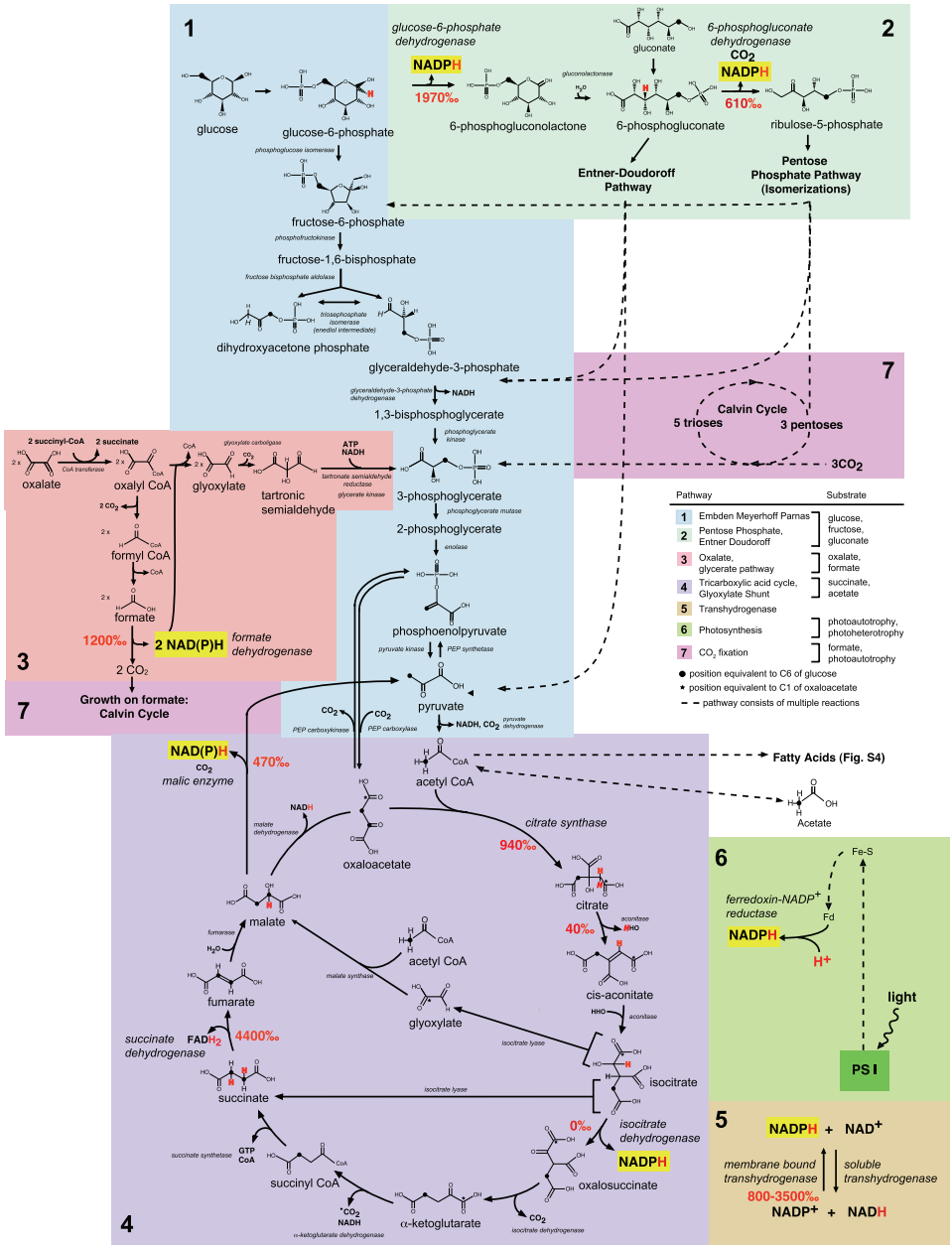

Fig. S5. Schematic summary of major central metabolic pathways highlighting the most important sources of NADPH reduction (refs. 1–5). (1) Embden–Meyerhoff–Parnas Pathway (glycolysis). (2) Oxidative pentose phosphate pathway and Entner–Doudoroff pathway (sugar degradation, glycolysis). (3) Oxalate degradation and assimilation via the glycerate pathway. (4) Tricarboxylic acid cycle and glyoxylate shunt. (5) Transhydrogenase. (6) Light reactions of photosynthesis. (7) Calvin cycle for CO_2 fixation. Reactions producing NADPH or potentially having strong influence on the isotopic composition of NADPH are highlighted. D/H fractionations (in permil notation), corresponding to isotope effects $^{H}k/^{D}k$ or $^{D}(V/K)$, are indicated by red numbers (6–10). Filled circles denote positions equivalent to C-6 of glucose and the methyl group of acetate. Filled stars denote the position equivalent to C-1 of oxaloacetate.

1. Gottschalk G (1986) *Bacterial Metabolism* (Springer-Verlag, New York).
2. Ingraham JL, Maaløe O, Neidhardt FC (1983) *Growth of the Bacterial Cell* (Sinauer, Sunderland, MA).
3. White D (2000) *The Physiology and Biochemistry of Prokaryotes* (Oxford Univ Press, New York).
4. Quayle JR (1961) Metabolism of C1 compounds in autotrophic and heterotrophic microorganisms. *Annu Rev Microbiol* 15:119–152.
5. Kornberg HL, Elsden SR (1961) The metabolism of 2-carbon compounds by microorganisms. *Adv Enzymol Relat Subj Biochem* 23:401–470.
6. Retey J, et al. (1970) Stereochemical studies of the exchange and abstraction of succinate hydrogen on succinate dehydrogenase. *Eur J Biochem* 14:232–242.
7. Thomson JF, Nance SL, Bush KJ, Szczepanik PA (1966) Isotope and solvent effects of deuterium on aconitase. *Arch Biochem Biophys* 117:65–74.
8. O'Leary MH (1989) Multiple isotope effects on enzyme-catalyzed reactions. *Annu Rev Biochem* 59:377–401.
9. Jackson JB, Peake SJ, White SA (1999) Structure and mechanism of proton-translocating transhydrogenase. *FEBS Lett* 464:1–8.
10. Lenz H, et al. (1971) Stereochemistry of *si*-citrate synthase and ATP-citrate-lyase reactions. *Eur J Biochem* 24:207–215.

Table S1. Relative abundances of fatty acids in bacterial cultures

	Fatty acid*											
Culture	12:0	14:1	14:0	15:0	16:1	16:0	cyc17	17:0	18:1	18:0	cyc19	19:0
Co1-I	—	—	—	—	0.39	0.38	—	—	0.22	—	—	—
Co1-II	—	—	—	—	0.35	0.39	—	—	0.25	0.01	—	—
Co1-III	—	—	—	—	0.36	0.36	0.01	—	0.27	0.01	—	—
Co1-IV	—	—	—	—	0.37	0.35	0.01	—	0.27	0.01	—	—
Co2-I	—	—	—	—	0.38	0.34	—	—	0.26	0.01	—	—
Co2-II	—	—	0.02	—	0.40	0.30	0.01	—	0.26	0.01	—	—
Co2-III	—	—	—	—	0.39	0.31	—	—	0.29	—	—	—
Co2-IV	—	—	—	—	0.37	0.33	—	—	0.29	0.01	—	—
Co3-I	—	—	—	—	0.40	0.34	—	—	0.25	0.01	—	—
Co3-II	—	—	—	—	0.40	0.34	—	—	0.25	0.01	—	—
Co3-III	—	—	—	—	0.39	0.36	—	—	0.24	0.01	—	—
Co3-IV	—	—	—	—	0.40	0.35	—	—	0.24	0.01	—	—
Co4-I	—	—	—	—	0.39	0.38	—	—	0.22	0.01	—	—
Co4-II	—	—	—	—	0.39	0.41	—	—	0.19	—	—	—
Co4-III	—	—	—	—	0.40	0.41	—	—	0.17	0.01	—	—
Co4-IV	—	—	0.01	—	0.39	0.42	—	—	0.17	0.01	—	—
Co5-I	—	—	0.03	—	0.39	0.33	—	—	0.25	0.01	—	—
Co5-II	—	—	—	—	0.45	0.38	—	—	0.16	—	—	—
Co5-III	—	—	—	—	0.43	0.40	—	—	0.17	—	—	—
Co5-IV	—	—	—	—	0.41	0.40	—	—	0.18	—	—	—
Co6-II	—	—	—	—	0.36	0.38	0.05	—	0.20	—	—	—
Co6-III	—	—	—	—	0.35	0.35	0.08	—	0.21	—	—	—
Co6-IV	—	—	—	—	0.41	0.36	0.06	—	0.17	—	—	—
Cn1-I	—	—	0.01	—	0.39	0.32	0.02	—	0.26	0.01	—	—
Cn2-I	—	—	0.02	—	0.42	0.29	0.01	—	0.25	0.01	—	—
Cn3-I	—	—	—	—	0.36	0.33	0.01	—	0.30	—	—	—
Cn4-I	—	—	0.01	—	0.43	0.39	—	—	0.18	—	—	—
Cn5-I	—	—	0.02	—	0.42	0.32	—	—	0.24	—	—	—
Cn6-I	—	—	0.02	—	0.39	0.34	—	—	0.23	0.01	—	—
Cn7-I	—	—	0.05	—	0.10	0.36	0.32	—	0.14	—	0.03	—
Ec1-I	0.01	—	0.04	0.01	0.21	0.45	0.13	0.01	0.14	—	0.01	—
Ec2-I	0.01	—	0.03	—	0.19	0.49	0.15	0.01	0.12	—	—	—
Ec3-I	—	—	0.02	—	0.16	0.50	0.18	—	0.11	0.02	0.01	—
Ec4-I	—	—	0.04	—	0.12	0.53	0.21	—	0.09	—	0.02	—
Ec5-I	0.02	—	0.04	0.01	0.20	0.43	0.11	—	0.17	—	0.01	—
Ec5-II	0.02	—	0.04	—	0.02	0.46	0.32	0.01	0.04	—	0.08	—
Ec5-III	0.02	—	0.04	0.01	0.15	0.44	0.16	0.01	0.15	—	0.01	—
Ec5-IV	0.02	—	0.04	0.01	0.01	0.50	0.22	0.01	0.15	—	0.02	—
Ec6-I	0.03	0.01	0.06	0.02	0.26	0.38	0.07	0.01	0.16	0.01	—	—
Ec6-II	0.03	0.01	0.07	0.02	0.29	0.38	0.04	0.01	0.15	—	—	—
Ec6-III	0.02	0.01	0.05	0.02	0.33	0.42	0.14	—	0.01	—	—	—
Rp1-I	—	—	—	—	0.01	0.08	—	—	0.53	0.21	0.15	0.02
Rp2-I	—	—	—	—	0.03	0.14	—	—	0.65	0.11	0.07	—
Rp3-I	—	—	—	—	0.03	0.15	—	—	0.69	0.10	0.01	—

*12:0, lauric acid; 14:1, myristoleic acid; 14:0, myristic acid; 15:0, pentadecanoic acid; 16:1, palmitoleic acid; 16:0, palmitic acid; cyc17, cyclopropyl-heptadecanoic acid; 17:0, heptadecanoic acid; 18:1, oleic acid; 18:0, stearic acid; cyc19, cyclopropyl-nonadecanoic acid; 19:0, nonadecanoic acid. Relative abundances are calculated from TIC peak areas of FAMEs as the fraction of total quantified fatty acids.

Table S2. Measured δD values of fatty acids and culture media water

		Fatty Acid*									
Culture	$n^{\dagger}$	16:1	σ	16:0	σ	cyc17	σ	18:1	σ	18:0	σ	Medium, δD_w
Co1-I	1	−356	—	−343	—	—	—	−338	—	—	—	−68.6
Co1-II	1	−281	—	−266	—	—	—	−260	—	—	—	44.6
Co1-III	1	−219	—	−198	—	—	—	−193	—	—	—	130.3
Co1-IV	1	−174	—	−148	—	—	—	−140	—	—	—	218.3
Co2-I	1	−362	—	−355	—	—	—	−342	—	—	—	−68.6
Co2-II	1	−291	—	−270	—	—	—	−269	—	—	—	44.6
Co2-III	1	−240	—	−212	—	—	—	−215	—	—	—	130.3
Co2-IV	1	−176	—	−143	—	—	—	−131	—	—	—	218.3
Co3-I	1	−344	—	−322	—	—	—	−319	—	—	—	−68.6
Co3-II	1	−269	—	−246	—	—	—	−239	—	—	—	44.6
Co3-III	1	−191	—	−170	—	—	—	−167	—	—	—	130.3
Co3-IV	1	−154	—	−130	—	—	—	−123	—	—	—	218.3
Co4-I	1	38	—	92	—	—	—	76	—	—	—	−68.6
Co4-II	1	93	—	149	—	—	—	129	—	—	—	44.6
Co4-III	1	129	—	187	—	—	—	167	—	—	—	130.3
Co4-IV	1	190	—	263	—	—	—	234	—	—	—	218.3
Co5-I	2	64	1.7	109	3.0	—	—	77	0.8	—	—	−64.3
Co5-II	3	176	1.0	219	1.4	—	—	205	1.6	—	—	41.1
Co5-III	3	235	2.5	282	1.2	—	—	266	2.8	—	—	121.1
Co5-IV	3	296	3.6	331	4.2	—	—	326	5.0	—	—	214.1
Co6-II	3	106	1.3	166	1.1	—	—	128	4.1	—	—	41.1
Co6-III	3	163	0.7	226	1.4	—	—	184	0.7	—	—	121.1
Co6-IV	3	238	1.6	302	3.2	—	—	258	1.8	—	—	214.1
Cn1-I	4	−298	3.5	−294	3.5	—	—	−287	8.2	—	—	−68.3
Cn2-I	2	−137	0.1	−101	1.4	—	—	−110	2.1	—	—	−65.5
Cn3-I	2	−124	1.9	−124	3.4	—	—	−109	4.1	—	—	−68.1
Cn4-I	4	−12	2.2	26	3.0	—	—	8	5.8	—	—	−64.4
Cn5-I	4	71	2.1	127	11.8	—	—	101	1.8	—	—	−68.5
Cn6-I	2	51	1.7	89	1.5	—	—	62	0.7	—	—	−68.6
Cn7-I	2	−35	2.6	−3	0.5	−11	1.9	−34	2.2	—	—	−68.6
Ec1-I	2	−176	2.7	−178	0.3	−160	2.8	−173	2.2	—	—	−61.9
Ec2-I	2	−196	4.3	−190	3.3	−166	1.4	−187	4.6	—	—	−62.2
Ec3-I	4	−124	3.8	−120	5.8	−112	3.7	−108	5.2	—	—	−68.1
Ec4-I	2	−23	2.2	−12	3.1	−7	0.7	−5	0.5	—	—	−62.4
Ec5-I	2	−197	0.0	−180	3.3	−178	2.7	−183	2.7	—	—	−60.0
Ec5-II	2	−122	10.4	−128	1.1	−121	1.3	−122	0.6	—	—	49.9
Ec5-III	2	−68	1.8	−44	1.4	−52	0.7	−44	0.5	—	—	152.0
Ec5-IV	2	30	0.4	57	0.2	41	1.2	50	3.2	—	—	314.0
Ec6-I	2	−152	0.6	−143	0.0	−139	1.4	−121	0.4	—	—	−60.0
Ec6-II	2	−98	0.3	−83	1.6	−116	2.9	−61	0.7	—	—	49.9
Ec6-III	2	−58	3.4	−34	0.5	−70	4.9	−20	7.1	—	—	152.0
Rp1-I	2	—	—	−87	1.4	—	—	−77	4.0	−37	0.5	−53.6
Rp2-I	2	−169	3.6	−185	1.4	—	—	−173	2.1	−157	1.4	−53.6
Rp3-I	2	—	—	−220	0.9	—	—	−229	1.2	−208	1.2	−53.6

*Fatty acid structures for corresponding abbreviations are listed in Table S1. Tabulated values are the average δD values for replicate analyses, in permil. Values of σ are calculated from replicate analyses.

†Number of replicate measurements for fatty acids

Table S3. Coefficients for regression of R_I on R_W and their standard errors (SE). Intercepts and their standard errors are x10^6

	16:1					16:0					18:1				
Cultures	Slope	SE	Intercept	SE	R^2	Slope	SE	Intercept	SE	R^2	Slope	SE	Intercept	SE	R^2
Co1-I,II,II,IV	0.64	0.03	7.22	4.77	1.00	0.69	0.03	2.83	4.77	1.00	0.70	0.02	1.72	3.48	1.00
Co2-I,II,II,IV	0.64	0.02	6.25	3.21	1.00	0.73	0.01	−5.70	2.13	1.00	0.72	0.05	−3.60	8.88	0.99
Co3-I,II,II,IV	0.69	0.06	3.04	10.25	0.98	0.69	0.05	5.97	8.62	0.99	0.70	0.04	4.92	7.50	0.99
Co4-I,II,II,IV	0.52	0.04	85.80	6.30	0.99	0.58	0.06	85.07	10.57	0.98	0.54	0.05	88.72	8.85	0.98
Co5-I,II,II,IV	0.83	0.07	46.55	12.18	0.99	0.80	0.09	58.07	14.58	0.98	0.89	0.10	40.34	16.90	0.98
Co6-II,II,IV	0.76	0.03	47.99	4.45	1.00	0.79	0.02	53.88	2.91	1.00	0.75	0.03	53.98	4.62	1.00
Ec5-I,II,III,IV	0.60	0.02	37.83	3.12	0.99	0.65	0.04	31.70	7.03	0.99	0.63	0.03	34.08	4.38	0.99
Ec6-I,II,III	0.44	0.03	67.19	5.28	0.99	0.52	0.02	57.99	3.42	0.99	0.48	0.04	67.41	6.42	0.99